A&A 405, 627–637 (2003)
DOI: 10.1051/0004-6361:20030645

Astronomy & Astrophysics

Angular dimensions of planetary nebulae⋆

R. Tylenda[1], N. Siódmiak[1], S. K. Górny[1], R. L. M. Corradi[2], and H. E. Schwarz[3]

[1] N. Copernicus Astronomical Center, Department for Astrophysics, Rabiańska 8, 87–100 Toruń, Poland
[2] Isaac Newton Group of Telescopes, Apartado de Correos 321, 38700 Sta. Cruz de La Palma, Spain
[3] CTIO/NOAO, Casilla 603, La Serena, Chile

Received 28 May 2002 / Accepted 23 April 2003

Abstract. We have measured angular dimensions of 312 planetary nebulae from their images obtained in Hα (or Hα + [NII]). We have applied three methods of measurements: direct measurements at the 10% level of the peak surface brightness, Gaussian deconvolution and second-moment deconvolution. The results from the three methods are compared and analysed. We propose a simple deconvolution of the 10% level measurements which significantly improves the reliability of these measurements for compact and partially resolved nebulae. Gaussian deconvolution gives consistent but somewhat underestimated diameters compared to the 10% measurements. Second-moment deconvolution gives results in poor agreement with those from the other two methods, especially for poorly resolved nebulae. From the results of measurements and using the conclusions of our analysis we derive the final nebular diameters which should be free from systematic differences between small (partially resolved) and extended (well resolved) objects in our sample.

Key words. planetary nebulae: general

1. Introduction

The angular dimensions belong to the most fundamental observational data for planetary nebulae (PNe). They are required if one wants to study important PN parameters such as linear dimensions, lifetimes, surface brightnesses. Several methods for determining distances or estimating nebular masses rely on observational measurements of the PN diameters. Also studies of the observed evolution of PNe and their central stars often use the angular PN diameters as one of the crucial observational data.

PN dimensions have been measured since the very beginning of research interest in these objects and the list of papers with resultant values is very long. Consequently, for almost all the known PNe we have information about their angular dimensions, see e.g. the ESO-Strasbourg Catalogue (Acker et al. 1992). However the data from many existing catalogues and databases should be used with caution. They have usually been compiled from numerous different sources based on different observational techniques and methods. Therefore the resulting data for different objects are not always comparable. For many PNe the diameters taken from different observational sources can differ by a factor of a few.

The problem is that different observational techniques and/or different methods for measuring dimensions give different results for many PNe. In the case of well resolved and fairly symmetric nebulae with a well defined outer rim the problem is simple and different methods give consistent results. Most of the PNe have, however, complex structures, soft outer boundaries, and low surface brightness emission extending to large distances. If one measures the maximum extension of the nebular emission in an image, as it has often been done while determining PN dimensions, than the result depends on how deep the image has been made. A reasonable solution in order to get results comparable for all objects is to measure nebular extension at a given level of surface brightness, e.g. at 10% of the maximum value.

Another problem arises in the case of small PNe when the nebular diameter is comparable to the angular resolution of the instrument. The observed image is then a convolution of an intrinsic nebular image and the instrumental profile. It has to be deconvolved in order to get a meaningful result. It is usually done using the so-called Gaussian deconvolution. The disadvantage of this method is that one has to adopt a shape of the intrinsic surface brightness distribution and the result depends on this assumption. The problem of determining dimensions of partially resolved nebulae has recently been discussed by van Hoof (2000). He has made a thorough model analysis of different methods for measuring partially resolved nebulae.

The question that arises, and which is important for using the measured dimensions in extensive, systematic studies of PNe, is to what extent the results from different methods are comparable. For instance, do the results from direct measurements at the 10% contour for extended nebulae mean the

Send offprint requests to: N. Siódmiak,
e-mail: alexan@ncac.torun.pl

⋆ Table 1 is only available in electronic form at
http://www.edpsciences.org

same as the values from a deconvolution method for compact objects? If the PNe were close to model nebulae studied by van Hoof (2000) the answer would be: yes, they measure more or less the same. However, real nebulae are often much different from the model ones and the answer is not a priori clear. We attempt to answer the above question in this paper.

In recent years, a number of observational surveys for studying PN structures and dimensions have been done. As surveys in radio wavelengths those of Aaquist & Kwok (1990) and Zijlstra et al. (1989) should be mentioned. Over 400 PNe have been observed in these two surveys, mostly at 5 GHz. PN diameters have been determined either from a 10% contour level (for well resolved nebulae) or from a Gaussian deconvolution (for partially resolved objects). Recent optical surveys can be found in Schwarz et al. (1992), Manchado et al. (1996), and Górny et al. (1999) where about 600 PNe have been observed. However, the PN dimensions given in these three catalogues usually refer to the maximum extension of the recorded emission. As the ratio of the maximum to faintest recorded surface brightness can vary by a large factor from one image to another these diameters do not measure the same for all the objects in the catalogues.

We have measured angular dimensions for 312 PNe. One of the goals is to provide a homogeneous set of PN diameters, i.e. values which mean the same, as much as possible, for all the objects in the sample. We have applied direct measurements at 10% of the peak surface brightness as well as deconvolution methods. The results have been used to investigate reliability of the methods and for comparative studies of the results from different methods. This helped us to obtain a homogeneous set of the PN diameters for the whole sample without important systematic differences between compact and extended nebulae.

2. Observational material

The observational material used in this paper is, in principle, the same as in Schwarz et al. (1992) and Górny et al. (1999). These are images of mostly southern PNe taken with the NTT and other telescopes at the ESO. For our measurements we have used only images in Hα (or Hα + [NII]). This has been done in order to have a uniform set of data and to avoid possible ionization stratification effects in the results which could have appeared if we had used, for instance, [OIII] images.

3. Methods of measurements

We have applied three methods of measuring PN dimensions. First one is a direct measurement of the nebular diameter at a level of 10% of the peak surface brightness, $\Theta_{10\%}$, from the PN image. As the nebulae in majority are not spherically symmetric we have measured two diameters along perpendicular axes. One of the axes was directed along the longest extension of the nebular emission.

Second method is the Gaussian deconvolution. The full width at half-maximum (FWHM) values, Φ, have been obtained from a two-dimensional Gaussian fitting to the observed PN image. Before fitting the background has been subtracted from the image. The same applied to field stars allowed us to derive the FWHM of the resolution profile, Φ_b. The deconvolved FWHM diameter, Φ_d, can then be obtained from

$$\Phi_d = \sqrt{\Phi^2 - \Phi_b^2}. \quad (1)$$

In order to get an estimate of the real nebular diameter, Φ_d has to be multiplied by a conversion factor which is a function of the observational resolution, Φ_d/Φ_b, and the adopted intrinsic surface brightness distribution of the nebula. Details of calculating the conversion factor for a constant surface brightness disc and constant emissivity shells can be found in van Hoof (2000).

Third method is the so-called second-moment deconvolution. This is an analogous method to the Gaussian deconvolution but the FWHM is determined from the second moment of the surface brightness distribution. The advantage of this method is that, unlike Gaussian deconvolution, the conversion factor is independent of the resolution of the observations. Details of applying second-moment deconvolution can be found in van Hoof (2000).

It is well known that the first method fails for small objects and therefore it is usually applied to well resolved nebulae. The deconvolution methods, on the contrary, are usually applied to small, partially resolved nebulae. In this paper we have, however, attempted to apply all the three methods to all the PNe in our sample. This has been done in order to be able to compare different methods and to study systematic differences between results from them.

4. Results of measurements

Table 1 presents the results of direct measurements done on our PN images. Following suggestions of van Hoof (2000) we give raw data from the deconvolution methods, i.e. the deconvolved FWHM, Φ_d, and the image resolution, Φ_b. Our final angular diameters of the PNe are given in Table 2. They are based on the measurements reported in Table 1 as well as on the discussion of the results from different methods presented in Sect. 5.

Column (1) in Table 1 gives the PNG number of the object while its usual name is in Col. (2). Column (3) gives the number of a figure showing the PN image in the original papers: "s" and "g" stand for Schwarz et al. (1992) and Górny et al. (1999), respectively. The deconvolved FWHM, Φ_d, and the resolution size, Φ_b, from the Gaussian fit are in Cols. (4) and (5), respectively. The same but from the second-moment method can be found in Cols. (6) and (7). The results of direct measuremets at 10% level are given in Col. (8). Some PNe have relatively deep images and the nebular emission extends well beyond the 10% contour. In this cases we have also measured the dimensions of the 3σ emission level above the background. The results are in Col. (9). Column (10) gives the percentage of the 3σ level in the peak surface brightness. All the measurement results are in arcsec.

For some objects the deconvolution methods do not work well and Table 1 does not give results in these cases. It has usually happened when the nebula was extended with complex structures and/or had a strong central star or several field stars superimposed on the PN image. In these cases the numerical

procedure fitting Gaussian or calculating moments either has failed or has given spurious results, or has just measured a star (central or one of the field stars). Note that the Gaussian fit fails more often that the second-moment method, particularly for larger nebulae.

Not all the objects published in Schwarz et al. (1992) and Górny et al. (1999) appear in Table 1. Some PNe were too faint in the images or larger than the image frame so meaningful measurements have not been possible. On the other hand, images for a few objects (those with no entry in Col. (3) in Table 1) have not been published. For most of these objects their images (although obtained with different equipement) can be found in Manchado et al. (1996).

For a few objects we had two images from independent observations. We give results from both images separately in two consecutive rows in Table 1 in these cases.

5. Comparison of the methods

In this section we compare the results from the three methods used to measure the PN dimensions. The aim is to study systematic effects between different methods. This will allow us to work out a procedure for deriving a consistent set of PN dimensions for all the objects, i.e. those well resolved as well as partially resolved, in our sample.

5.1. Deconvolution methods: Gaussian versus second-moment

As discussed above, both, Gaussian fitting and second-moment calculations have been applied to measure the FWHM of the resolution profile, Φ_b, on our images. The results are given in Cols. (5) and (7) of Table 1. Both methods should give the same result if the instrumental profile is Gaussian. As can be seen from Table 1 this is essentially the case. The mean value and the standard deviation of the ratio Φ_b(Gauss)/Φ_b(s-m) calculated from the data in Table 1 is 0.965 ± 0.094. Thus the basic assumption of the deconvolution methods, namely Gaussian resolution profile, is satisfied in our observational material.

The final results of the Gaussian and second-moment deconvolution methods are compared in Fig. 1. The figure plots the ratio of the angular diameters, Θ, derived from the two methods versus the ratio of the deconvolved FWHM, Φ_d, to the resolution size, Φ_b, (i.e. parameter β in van Hoof 2000) obtained from the Gaussian fit. The values plotted in Fig. 1 are geometric means of the values obtained from the two-dimensional measurements reported in Table 1. While deriving Θ a surface brightness distribution from a constant emissivity sphere model (shell 0.0 in van Hoof's notation) has been adopted for calculating the conversion factors. Note, however, that the diagram shown in Fig. 1 depends only weakly on the adopted surface brightness distribution.

As can be seen from Fig. 1, the two deconvolution methods do not give the same result for the bulk of objects. The second-moment method tends to give larger diameters than the Gaussian deconvolution. In the case of compact nebulae, i.e. when the Gaussian deconvolution gives $\log \Phi_d/\Phi_b \lesssim 0.0$, the difference becomes particularly important and increases with decreasing PN size (as measured from the Gaussian deconvolution). Note that the vertical scatter of the points in Fig. 1, tends to become larger for more extended nebulae. On average $\log \Theta_{\rm Gauss}/\Theta_{\rm s-m}$ for objects with $\log \Phi_d/\Phi_b \geq 0.0$ is -0.096 ± 0.071 (mean and standard deviation). When adopting a shell-like model this value would go down and for an infinitely thin shell (limit 1.0 in van Hoof's notation) it would become -0.125 ± 0.070. If a constant surface brightness disc is adopted the figures would be -0.108 ± 0.071.

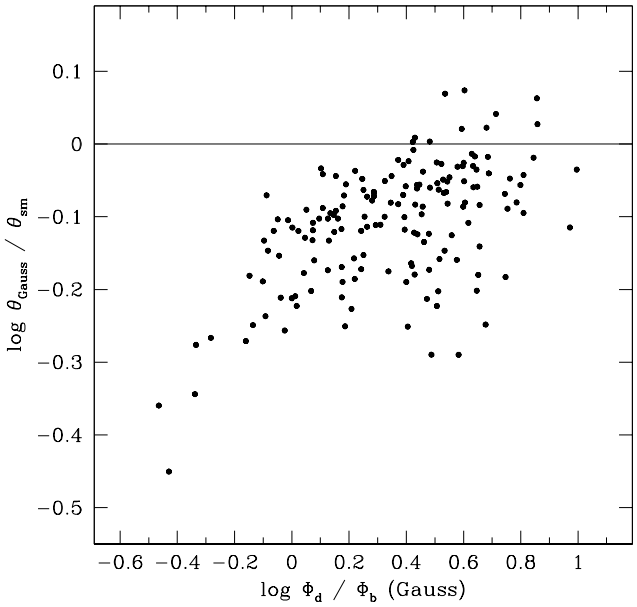

Fig. 1. Comparison of the results from the Gaussian deconvolution and the second-moment deconvolution. The ratio of the angular diameters, Θ, derived from the two methods is plotted versus the ratio of the deconvolved FWHM, Φ_d, to the resolution size, Φ_b, obtained from the Gaussian fit. A constant emissivity sphere model has been adopted while deriving Θ in both methods.

5.2. Gaussian deconvolution versus direct measurements at the 10% level

Figure 2 compares the results from the Gaussian deconvolution with the 10% contour measurements. Similarly as Fig. 1, it shows the ratio of the PN diameters versus the Gaussian Φ_d/Φ_b ratio. Again, the plotted values are geometric means from the measurements in Table 1. While obtaining the diameters from the Gaussian method the constant emissivity sphere model has been adopted. Note that the diagram in Fig. 2 depends on the adopted surface brightness distribution more significantly than Fig. 1. The general pattern of the diagram remains the same but the points can shift vertically.

Figure 2 shows an increasing discrepancy between the 10% diameter and the diameter from the Gaussian deconvolution with the decreasing value of Φ_d/Φ_b. This is an expected effect and is due to an overestimate of the PN diameter from the direct measurements for partially resolved PNe. Note, however, that a tight correlation seen in Fig. 2 for $\log \Phi_d/\Phi_b \lesssim 0.0$ is partly spurious. For Φ approaching Φ_b the *y*-axis in Fig. 2 tends to plot a reversal of the value plotted in the *x*-axis.

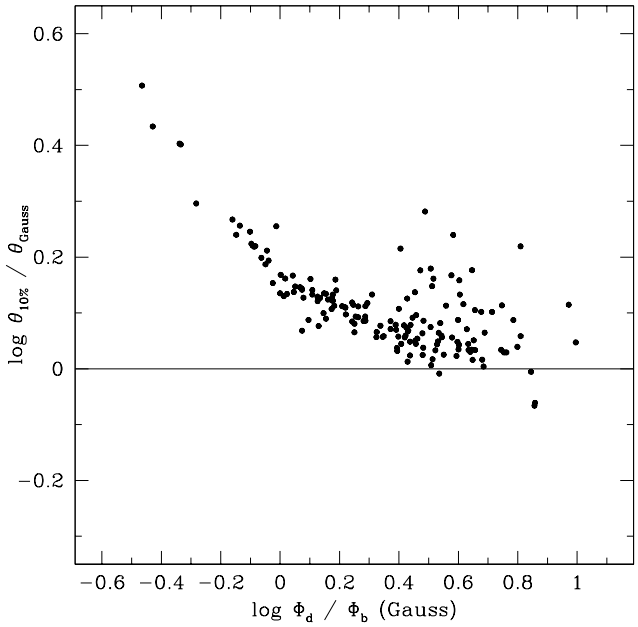

Fig. 2. Comparison of the results from the 10% contour measurements and the Gaussian deconvolution. The ratio of the angular diameters, Θ, derived from the two methods is plotted versus the ratio of the deconvolved FWHM, Φ_d, to the resolution size, Φ_b, obtained from the Gaussian fit. A constant emissivity sphere model has been adopted while deriving Θ in the Gaussian deconvolution.

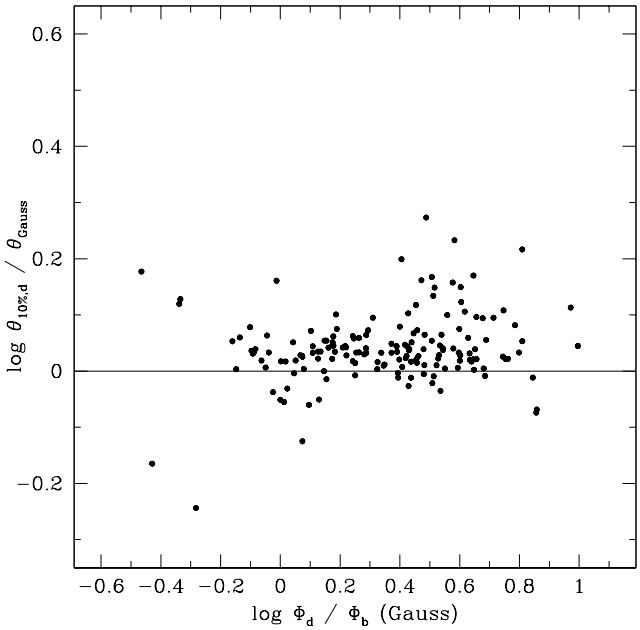

Fig. 3. The same as Fig. 2 but using the deconvolved 10% diameter, $\Theta_{10\%,d}$, calculated from Eq. (2).

For small nebulae the diameters from the 10% contour would be more accurate if determined from deconvolved images. We have not attempted to apply this rather cumbersome procedure to our images. Instead we have found that a significant improvement of the 10% diameter can be obtained using a formula analogous to the standard FWHM Gaussian deconvolution (Eq. (1)) but relevant to a 10% level of the maximum, i.e.

$$\Theta_{10\%,d} = \sqrt{\Theta_{10\%}^2 - (1.823\,\Phi_b)^2}. \qquad (2)$$

We will call $\Theta_{10\%,d}$ the deconvolved 10% diameter.

Figure 3 shows the same as Fig. 2 but using $\Theta_{10\%,d}$ instead of $\Theta_{10\%}$. Unlike in Fig. 2, the distribution of the points in Fig. 3 does not show any significant trend with Φ_d/Φ_b. This demonstrates that Eq. (2) allows to significantly improve the reliability of the PN dimension estimate from the 10% contour measurements for small, partially resolved nebulae. $\Theta_{10\%,d}$ seems to be an estimate of compact PN diameters as reliable as that from the Gaussian deconvolution.

However, as can be seen from Fig. 3, the Gaussian deconvolution tends to underestimate the PN dimensions compared to the 10% deconvolved diameters. Note that the value of this systematic difference depends on the surface brightness distribution adopted in the Gaussian method. It is smallest for the constant emissivity sphere, i.e. for the case presented in Fig. 3, and largest for the infinitely thin shell model.

Figure 3 suggests that the two methods give the most consistent results for rather compact but not too small nebulae, i.e. having $-0.2 \lesssim \log\Phi_d/\Phi_b \lesssim 0.3$. The mean value of $\log\Theta_{10\%,d}/\Theta_{Gauss}$ for these objects in Fig. 3 is 0.028 ± 0.041. For an infinitely thin shell (limit 1.0 in van Hoof's notation) and a constant surface brightness disc the result would be 0.159 ± 0.043 and 0.085 ± 0.042, respectively.

A greater discrepancy of the results for $\log\Phi_d/\Phi_b > 0.3$ can be seen from Fig. 3. The mean values of $\log\Theta_{10\%,d}/\Theta_{Gauss}$ derived for these objects are: 0.052 ± 0.062 (sphere), 0.195 ± 0.062 (thin shell), and 0.115 ± 0.062 (disc). These nebulae show resolved structures on the images and their surface brightness distributions are usually far from a Gaussian. Therefore a Gaussian fitting to such objects gives uncertain, sometimes even spurious, results.

Because of low statistics, no meaningful analysis can be done for the region $\log\Phi_d/\Phi_b < -0.2$. A large scatter of the points is certainly due to increasing sensitivity of the results to the observational uncertainties (quadratic subtraction of two nearly equal values).

5.3. Second-moment deconvolution versus direct measurements at 10% level

Figures 4 and 5 compare the results from the 10% level measurements and the second-moment deconvolution. Figure 4 is analogous to Fig. 2 and uses "raw" measurements from the 10% contour. A tendency of overestimating diameters for compact PNe from the 10% measurements can be seen in Fig. 4. It is, however, much less conspicuous than in Fig. 2. The reason is that, as discussed in Sect. 5.1, for partially resolved PNe the second-moment deconvolution results in larger diameters than the Gaussian deconvolution.

The deconvolved 10% diameter, using Eq. (2) and Φ_b from the second-moment calculations, have been applied in the diagram shown in Fig. 5. As the deconvolution of the 10% diameter most affects the results for compact nebulae the positions of these objects are significantly shifted down in Fig. 5 comparing to Fig. 4.

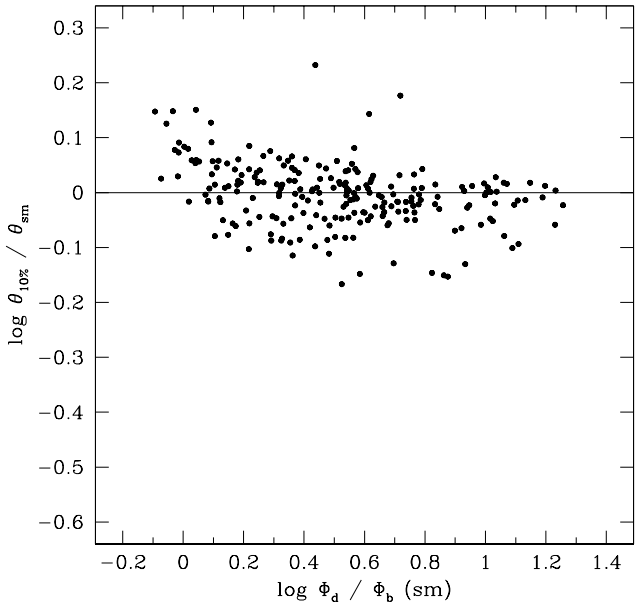

Fig. 4. Comparison of the results from the 10% contour measurements and the second-moment deconvolution. The ratio of the angular diameters, Θ, derived from the two methods is plotted versus the ratio of the deconvolved FWHM, $\Phi_{\rm d}$, to the resolution size, $\Phi_{\rm b}$, obtained from the moment calculations. A constant emissivity sphere model has been adopted while deriving Θ in the second-moment deconvolution.

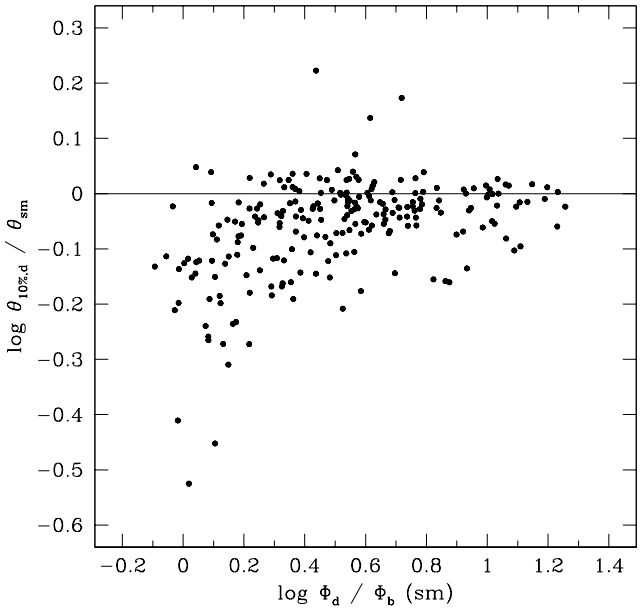

Fig. 5. The same as Fig. 4 but using the deconvolved 10% diameter, $\Theta_{10\%,\rm d}$, calculated from Eq. (2).

Figure 5 shows that the second-moment deconvolution usually overestimates the PN size compared to the 10% contour measurements. For rather large nebulae, i.e. having $\log\Phi_{\rm d}/\Phi_{\rm b} \geq 0.3$ in Fig. 5, $\log\Theta_{10\%,\rm d}/\Theta_{\rm s-m}$ is -0.033 ± 0.061. The discrepancy increases for less resolved nebulae and for $\log\Phi_{\rm d}/\Phi_{\rm b} < 0.3$, $\log\Theta_{10\%,\rm d}/\Theta_{\rm s-m}$ is -0.132 ± 0.115.

As the conversion factors in the second-moment deconvolution are independent of $\Phi_{\rm d}/\Phi_{\rm b}$ adopting the infinitely thin shell model would shift all the points in Fig. 5 upwards by factor 0.111. For the uniform disc model the shift would be of factor 0.048. By the same factors would respectively increase the mean values of $\log\Theta_{10\%,\rm d}/\Theta_{\rm s-m}$ (obviously, the standard deviations would remain the same).

5.4. Testing the methods on degraded PN images

One of the main problems in the present study is to find which method(s) gives reliable diameter estimates for partially resolved nebulae. The analysis discussed in the previous subsections shows that the deconvolved 10% diameter and the Gaussian deconvolution give relatively consistent results down to rather poorly resolved objects, although the Gaussian deconvolution systematically underestimates the PN diameter compared to the measurements of the 10% contour. The value of this underestimate depends on the model nebula adopted in the Gaussian deconvolution. On the other hand, the second-moment deconvolution seems to become unstable for compact objects as suggested by an increasing scatter of points in Fig. 5 for less and less resolved nebulae. However, we cannot be sure that this interpretation is correct. Nor we can say which method and when breaks to give reliable results. The reason is that we can compare only the results from different methods but we do not know what real diameters of poorly resolved nebulae are.

We have attempted to clarify the above problems by applying the methods of diameter measurements to some of our images artificially degraded to worse and worse seeing conditions, i.e. convolved with a larger and larger Gaussian profile. From the original images we know the true PN sizes so we can compare them to the results from different methods applied to less and less resolved PN images.

Although the idea is simple it could have been applied to a limited number of our images only. Obviously we have to consider rather well resolved nebulae but not too much. The object has to be several times smaller than the image size. Otherwise the image frame can impose an important cutoff when the image is convolved with a Gaussian having FWHM comparable to the PN size. The nebula has to be well exposed so its image keeps a good contrast while beeing spread over larger and larger surface. There cannot be too many bright field stars, otherwise they merge with the PN image in the convolution process. It is also desirable that among the objects investigated different morphologies are represented.

We present the results of the procedure applied to images of 5 PN, i.e. (in paranthesis usual names and morphological descriptions are given) 021.8–00.4 (M 3-28; bipolar, butterfly-like), 174.2–14.6 (H 3-29; ring-like but strongly asymmetric with one strong blob), 285.7–14.9 (IC 2448; round with a halo), 286.3–04.8 (NGC 3211; ring-like with two blobs), and 345.2–08.8 (Tc 1; round with an irregular halo). The selected objects have diameters between 10 and 20 arcsec. The original images have been obtained with a seeing varying from 0.5 to 2.5 arcsec. We have used our deconvolved 10% diameters from original images as true PN diameters for comparison with the results from degraded images (note that the deconvolution has introduced only minor corrections to the 10% contour measurements in these cases). The original images have been

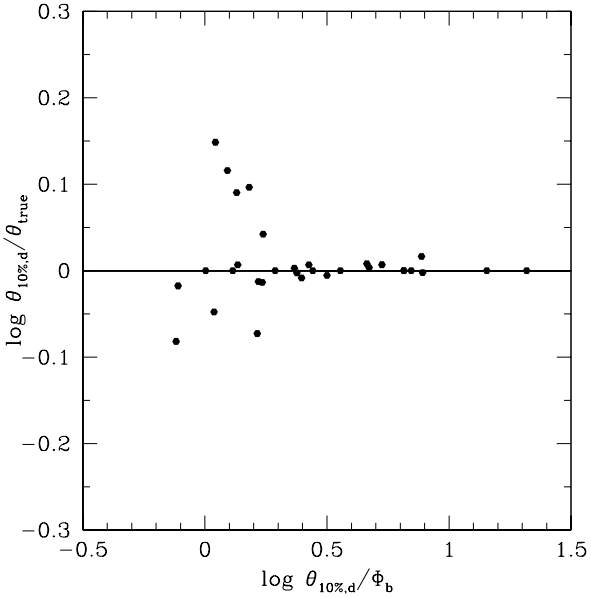

Fig. 6. Results of the 10% contour measurements on the degraded PN images. $\Theta_{10\%,d}$ and Φ_b are the deconvolved 10% diameter and the seeing size, respectively, measured from the degraded images. Θ_{true} is the deconvolved 10% diameter from the original (non-degraded) images.

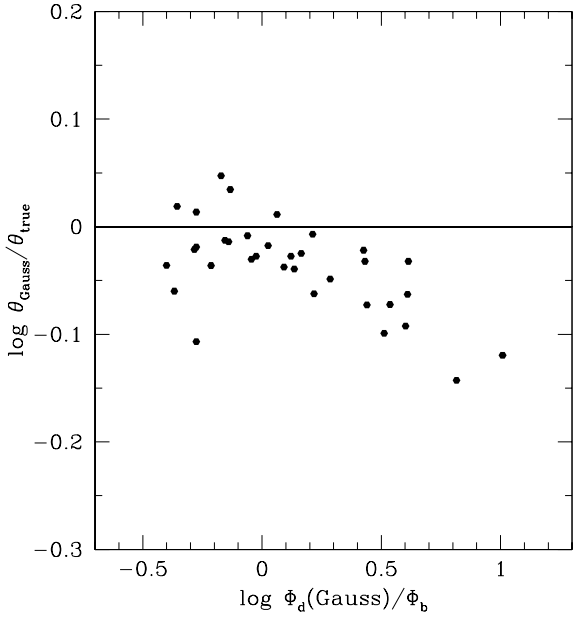

Fig. 7. The same as Fig. 6 but for the Gaussian deconvolution adopting a constant emissivity sphere model. Θ_{true} is the deconvolved 10% diameter from the original (non-degraded) images.

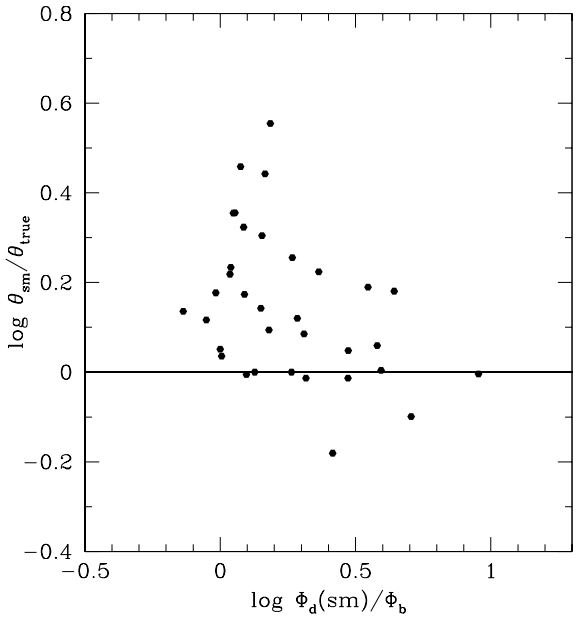

Fig. 8. The same as Fig. 6 but for the second-moment deconvolution adopting a constant emissivity sphere model. Θ_{true} is the deconvolved 10% diameter from the original (non-degraded) images.

convolved with a Gaussian having FWHM increasing from 2.5 to 20.0 arcsec. Then our three methods have been applied to the resulting images.

We note that the results from measurements on the degraded images reproduce very well the general trends seen in Figs. 1–5.

In Fig. 6 the results of the deconvolved 10% diameter method applied to the degraded images are compared to the deconvolved 10% diameter from the original (non-degraded) images (Θ_{true}). From this figure we can conlude that the deconvolved 10% diameter measures very well the PN size down to $\log\Theta_{10\%,d}/\Phi_b \simeq 0.3$. This limit is practically equivalent to $\log\Phi_d(\mathrm{Gauss})/\Phi_b \simeq 0.05$. Below this value the method becomes unstable.

Results of the Gaussian deconvolution applied to the degraded images are presented in Fig. 7. A constant emissivity sphere model has been adopted. We see that for well resolved nebulae the Gaussian deconvolution underestimates the PN diameter. This is consistent with the trend seen in Fig. 3. For $\log\Phi_d/\Phi_b \lesssim 0.3$ the underestimate is smaller, again similar as in Fig. 3. For all the points with $\log\Phi_d/\Phi_b < 0.3$ in Fig. 7 the mean value and the standard deviation of $\log\Theta_{Gauss}/\Theta_{true}$ are -0.021 ± 0.032. This result is very close to the value -0.028 ± 0.041 of $\log\Theta_{Gauss}/\Theta_{10\%,d}$ found in Sect. 5.2 for objects having $-0.2 \lesssim \log\Phi_d/\Phi_b \lesssim 0.3$ in Fig. 3. For $\log\Phi_d/\Phi_b \lesssim -0.2$ in Fig. 7 the scatter increases which suggests that the Gaussian deconvolution becomes then unstable. Comparison of Figs. 7 and 6 seems to indicate that the Gaussian deconvolution gives somewhat more stable results than the deconvolved 10% diameter for objects having $\log\Theta_{10\%,d}/\Phi_b \leq 0.3$ or, equivalently, $\log\Phi_d(\mathrm{Gauss})/\Phi_b \leq 0.05$. A better statistics would be required to clarify this point.

The results of the test of the second-moment deconvolution are presented in Fig. 8. A constant emissivity sphere model has been adopted. The figure shows that the second-moment deconvolution gives uncertain estimates of the PN diameters, especially for partially resolved nebulae ($\log\Phi_d/\Phi_b < 0.3$). Adopting a shell or disc model in the deconvolution would decrease the systematic difference between Θ_{s-m} and Θ_{true} in Fig. 8 but the uncertainity (scatter of the points) would remain

the same. Our experience suggests that this method is sensitive to faint outer structures (halo, outer butterfly-like filaments) particularly in partially resolved nebulae.

6. PN diameters

One of the primary goals of our work is to obtain a homogeneous set of PN dimensions, a set of results which have, as far as possible, the same physical meaning for all the objects in our sample. As a primary method for deriving the PN dimensions we have adopted the direct measurements at the 10% level of the peak surface brightness. This seems to be the only reasonable method for well resolved nebulae. In order to account for the finite resolution in the case of smaller objects we have used the deconvolved 10% diameters, $\Theta_{10\%,d}$, instead of $\Theta_{10\%}$. As discussed in Sect. 5.4 $\Theta_{10\%,d}$ is reliable down to $\log \Theta_{10\%,d}/\Phi_b \simeq 0.3$. For the smallest objects when results from any method become more and more uncertain we have used $\Theta_{10\%,d}$ and the results from the Gaussian deconvolution. Following discussion in Sect. 5.4 we have prefered not to use the results from the second-moment deconvolution. In more detail our prescription is as follows.

For all the objects with $\log \Theta_{10\%,d}/\Phi_b \geq 0.3$ we have adopted $\Theta_{10\%,d}$. We have used Φ_b from Gaussian fit. For more compact objects, i.e. when $\log \Theta_{10\%,d}/\Phi_b < 0.3$ we have adopted a mean value from $\Theta_{10\%,d}$ and Θ resulting from the Gaussian deconvolution adopting the constant emissivity sphere model. In order to correct for the systematic underestimate of the Gaussian method, as discussed in Sects. 5.2 and 5.4, the Gaussian Θ have been multiplied by factor 1.06 before deriving the mean value.

The results are presented in Table 2. Columns 1 and 2 give the PNG numbers and the usual names, respectively. The diameters derived according to the above prescription are given in Col. 3. In the case of partially resolved objects having $\log \Theta_{10\%,d}/\Phi_b < 0.3$ only one value is given which is the geometric mean from the two dimension measurements. A colon indicates compact objects for which the Gaussian deconvolution resulted in a diameter different by more than 30% from the deconvolved 10% diameter. Objects practically unresolved in our images are marked with "stellar". For a few objects having two independent measurements in Table 1 mean values derived from them are given in Table 2.

We have compared the results from Table 2 with the diameters from our data base resulting from a compilation of the data published in the literature. This data base has originally been made for purposes of the Strasbourg-ESO catalogue (Acker et al. 1992). Its updated version has been described and used in Siódmiak & Tylenda (2001). The results of the comparison are shown in Fig. 9. In most cases the agreement is quite good although our measurements tend to give somewhat larger diameters than the values adopted from the literature. The mean value of the ratio of our diameters (from Table 2) to the compiled diameters is 1.24 with a standard deviation of 0.71. In some cases, however, the discrepancy is significant. For small nebulae a large scatter of the points in Fig. 9 is not surprising. Any measurement, VLA or optical, of a partially resolved nebulae gives an uncertain result. Significant discrepancies in

Table 2. Nebular diameters (in arcsec).

PN G	Main Name	diameter	
(1)	(2)	(3)	
000.1+17.2	PC 12	2.3 x	2.2
000.1-01.1	M 3-43	4.1 x	2.6
000.1-05.6	H 2-40	18.3 x	16.9
000.2-01.9	M 2-19	9.4 x	8.5
000.3+12.2	IC 4634	20.5 x	6.6
000.4-01.9	M 2-20	4.1 x	3.4
000.7+04.7	H 2-11	2.0	
001.0+01.9	K 1- 4	48.1 x	33.6
001.5-06.7	SwSt 1	5.6 x	5.2
002.0-13.4	IC 4776	8.5 x	4.0
002.2-06.3	H 1-63	3.8 x	3.2
002.2-09.4	Cn 1-5	7.4 x	7.4
002.4+05.8	NGC 6369	33.0 x	32.7
002.5-01.7	Pe 2-11	7.8 x	6.5
002.7-04.8	M 1-42	13.1 x	11.3
002.7-52.4	IC 5148-50	132.5 x	127.8
002.8+01.7	H 2-20	stellar	
003.1+02.9	Hb 4	11.1 x	6.8
003.1+03.4	H 2-17	4.8 x	3.9
003.5-02.4	IC 4673	22.0 x	15.2
003.5-04.6	NGC 6565	10.8 x	10.5
003.6-02.3	M 2-26	10.5 x	10.4
003.7+07.9	H 2- 8	11.9 x	6.7
003.8-04.5	H 2-41	9.3 x	9.2
003.8-17.1	Hb 8	0.8 :	
003.9-14.9	Hb 7	3.5	
004.0-11.1	M 3-29	9.7 x	8.6
004.8-22.7	He 2-436	3.6 x	2.8
004.9-04.9	M 1-44	6.0 x	5.4
005.0+03.0	Pe 1- 9	13.6 x	13.4
005.0-03.9	H 2-42	13.0 x	11.9
005.1-08.9	Hf 2-2	21.7 x	21.7
006.0+03.1	M 1-28	33.1 x	30.3
006.1+08.3	M 1-20	2.5 x	2.3
006.8-08.6	Al 1	15.00 x	12.3
007.2+01.8	Hb 6	7.7 x	6.8
008.0+03.9	NGC 6445	45.3 x	36.2
008.3-01.1	M 1-40	9.2 x	7.5
008.3-07.3	NGC 6644	4.4 x	4.3
009.4-05.0	NGC 6629	16.6 x	15.5
009.4-09.8	M 3-32	8.1 x	6.8
009.6+10.5	A 41	20.2 x	17.3
009.6+14.8	NGC 6309	22.8 x	12.4
009.6-10.6	M 3-33	7.4 x	7.3
010.7-06.4	IC 4732	1.4 :	
010.8+18.0	M 2- 9	37.0 x	11.0
010.8-01.8	NGC 6578	12.1 x	11.8
011.0-05.1	M 1-47	6.2 x	5.3
011.1+11.5	M 2-13	3.0 x	2.4
011.7-00.6	NGC 6567	8.1 x	6.4
011.9+04.2	M 1-32	9.1 x	8.0
012.5-09.8	M 1-62	4.8 x	4.6
013.0-04.3	Pe 2-14	5.5 x	5.3
013.3+32.7	Sn 1	5.9 x	5.0
014.6-04.3	M 1-50	4.2 x	3.9
016.4-01.9	M 1-46	12.1 x	11.3
017.6-10.2	A 51	59.2 x	59.0
017.9-04.8	M 3-30	19.1 x	18.4

Table 2. continued.

(1)	(2)	(3)
020.9-01.1	M 1-51	15.4 x 8.3
021.2-03.9	We 1-7	20.5 x 19.7
021.7-00.6	M 3-55	12.2 x 9.3
021.8-00.4	M 3-28	24.1 x 12.1
023.9-02.3	M 1-59	6.7 x 6.0
024.2+05.9	M 4- 9	47.9 x 42.6
024.3-03.3	Pe 1-17	14.7 x 7.6
025.8-17.9	NGC 6818	24.7 x 24.7
025.9-10.9	Na 2	6.3 x 5.7
027.3-03.4	A 49	54.1 x 38.2
027.7+00.7	M 2-45	9.4 x 7.6
028.0+10.2	WeSb 3	50.7 x 43.1
028.7-03.9	Pe 1-21	11.1 x 10.4
029.2-05.9	NGC 6751	24.1 x 23.2
030.8+03.4	A 47	17.5 x 12.3
031.0-10.8	M 3-34	7.4 x 6.4
033.0-05.3	A 55	56.8 x 52.3
033.1-06.3	NGC 6772	80.7 x 70.8
033.8-02.6	NGC 6741	9.1 x 6.5
034.5-06.7	NGC 6778	21.4 x 15.5
035.9-01.1	Sh 2- 71	132.4 x 74.9
037.5-05.1	A 58	44.7 x 33.7
037.7-34.5	NGC 7009	28.0 x 22.0
037.8-06.3	NGC 6790	4.4 x 3.4
038.1-25.4	A 70	45.2 x 37.8
038.2+12.0	Cn 3-1	5.7 x 4.6
039.5-02.7	M 2-47	6.9 x 4.9
040.3-00.4	A 53	31.9 x 31.1
042.9-06.9	NGC 6807	2.0 x 1.9
043.1+03.8	M 1-65	4.2 x 4.0
043.3+11.6	M 3-27	2.8 x 2.3
045.4-02.7	Vy 2-2	3.1 x 2.6
045.7-04.5	NGC 6804	58.3 x 48.6
046.4-04.1	NGC 6803	5.4 x 5.1
054.1-12.1	NGC 6891	13.5 x 12.7
061.4-09.5	NGC 6905	43.3 x 35.6
062.4-00.2	M 2-48	19.4 x 11.3
065.2-05.6	He 1- 6	40.5 x 21.5
066.7-28.2	NGC 7094	102.5 x 99.4
069.2+03.8	K 3-46	36.2 x 23.5
069.4-02.6	NGC 6894	56.4 x 53.3
118.8-74.7	NGC 246	260.4 x 226.7
161.2-14.8	IC 2003	10.0 x 8.1
171.3-25.8	Ba 1	39.8 x 38.3
174.2-14.6	H 3-29	23.8 x 18.8
189.1+19.8	NGC 2371-72	48.9 x 30.6
190.3-17.7	J 320	9.4 x 6.4
194.2+02.5	J 900	8.2 x 7.8
196.6-10.9	NGC 2022	27.9 x 25.5
197.2-14.2	K 1- 7	37.2 x 36.0
198.6-06.3	A 12	44.1 x 38.5
201.9-04.6	We 1-4	41.4 x 37.6
206.4-40.5	NGC 1535	33.3 x 32.1
212.0+04.3	M 1- 9	2.7
214.9+07.8	A 20	67.3 x 60.5
216.3-04.4	We 1-5	20.3 x 19.3
221.3-12.3	IC 2165	9.3 x 8.9
221.7+05.3	M 3- 3	16.6 x 15.8
224.9+01.0	We 1-6	60.9 x 58.4
226.4-03.7	PB 1	10.6 x 9.5

Table 2. continued.

(1)	(2)	(3)
226.7+05.6	M 1-16	7.7 x 5.5
228.8+05.3	M 1-17	3.8
229.6-02.7	K 1-10	51.3 x 46.0
231.4+04.3	M 1-18	34.9 x 32.9
231.8+04.1	NGC 2438	80.7 x 78.3
232.4-01.8	M 1-13	18.6 x 11.6
232.8-04.7	M 1-11	5.2 x 5.1
233.5-16.3	A 15	36.6 x 34.7
234.8+02.4	NGC 2440	58.9 x 25.1
234.9-01.4	M 1-14	5.7 x 5.2
236.7+03.5	K 1-12	44.1 x 36.4
238.9+07.3	Sa 2-21	40.3 x 34.4
239.6+13.9	NGC 2610	49.7 x 47.6
240.3-07.6	M 3- 2	12.3 x 9.1
242.6-11.6	M 3- 1	12.6 x 10.8
243.3-01.0	NGC 2452	18.3 x 12.4
245.4+01.6	M 3- 5	8.3 x 7.3
248.8-08.5	M 4- 2	8.2 x 7.1
249.0+06.9	SaSt 1- 1	1.2
250.3+00.1	A 26	37.5 x 36.7
252.6+04.4	K 1- 1	51.3 x 47.5
258.1-00.3	He 2- 9	5.9 x 4.7
259.1+00.9	He 2- 11	121.7 x 64.0
261.0+32.0	NGC 3242	31.5 x 30.7
261.9+08.5	NGC 2818	56.2 x 46.0
262.6-04.6	Wray 17-18	17.2 x 16.8
264.4-12.7	He 2- 5	3.8 x 3.6
265.7+04.1	NGC 2792	17.9 x 16.4
268.4+02.4	PB 5	1.7 x 1.6
272.1+12.3	NGC 3132	59.9 x 45.6
273.2-03.7	He 2- 18	16.4 x 13.7
274.3+09.1	Lo 4	41.6 x 38.9
274.6+02.1	He 2- 35	4.0 x 3.6
274.6+03.5	He 2- 37	26.1 x 22.1
275.0-04.1	PB 4	12.2 x 10.2
275.2-02.9	He 2- 28	10.8 x 10.0
275.2-03.7	He 2- 25	54.2 x 10.6
275.8-02.9	He 2- 29	16.0 x 11.8
277.1-03.8	NGC 2899	68.5 x 59.8
278.1-05.9	NGC 2867	14.4 x 13.9
279.6-03.1	He 2- 36	24.8 x 15.3
283.8+02.2	My 60	10.1 x 10.1
283.8-04.2	He 2- 39	12.4 x 12.2
283.9-01.8	Hf 4	29.1 x 21.0
285.4+02.2	Pe 2- 7	5.6 x 4.4
285.4-05.3	IC 2553	11.5 x 7.4
285.6-02.7	He 2- 47	4.9 x 4.4
285.7+01.2	Pe 1- 2	4.0 x 3.1
285.7-14.9	IC 2448	10.7 x 10.0
286.3-04.8	NGC 3211	16.1 x 15.9
288.4-02.4	Pe 1- 3	10.9 x 8.8
289.8+07.7	He 2- 63	3.0
291.4+19.2	ESO 320-28	30.4 x 27.2
291.6-04.8	IC 2621	4.0 x 3.6
291.7+03.7	He 2- 64	9.1 x 8.3
292.4+04.1	PB 8	6.6 x 6.5
292.6+01.2	NGC 3699	47.0 x 37.0
292.8+01.1	He 2- 67	5.2 x 2.8
293.6+01.2	He 2- 70	34.6 x 13.6
294.1+14.4	Lo 6	77.0 x 74.4

Table 2. continued.

(1)	(2)	(3)
294.6+04.7	NGC 3918	18.7 x 17.1
294.9-04.3	He 2- 68	2.5
296.3-03.0	He 2- 73	3.3 x 2.5
296.6-20.0	NGC 3195	39.5 x 33.8
297.4+03.7	He 2- 78	3.5
298.1-00.7	He 2- 77	25.4 x 14.1
298.2-01.7	He 2- 76	17.0 x 17.0
298.3-04.8	NGC 4071	72.4 x 52.7
299.0+18.4	K 1-23	64.3 x 56.4
299.5+02.4	He 2- 82	31.8 x 25.4
299.8-01.3	He 2- 81	7.3 x 6.5
300.2+00.6	He 2- 83	4.7 x 4.5
300.4-00.9	He 2- 84	35.8 x 23.7
300.5-01.1	He 2- 85	9.2 x 7.9
300.7-02.0	He 2- 86	3.2
304.5-04.8	IC 4191	5.3 x 4.5
304.8+05.1	He 2- 88	1.7
305.1+01.4	He 2- 90	3.2 x 3.1
306.4-00.6	Th 2- A	27.3 x 24.8
307.2-03.4	NGC 5189	163.4 x 108.2
307.2-09.0	He 2- 97	2.3
307.5-04.9	MyCn 18	17.3 x 9.8
308.6-12.2	He 2-105	41.5 x 40.7
309.0+00.8	He 2- 96	2.8
309.0-04.2	He 2- 99	27.9 x 23.4
309.1-04.3	NGC 5315	10.7 x 9.2
310.7-02.9	He 2-103	22.1 x 20.9
311.0+02.4	SuWt 2	86.5 x 43.4
311.4+02.8	He 2-102	11.7 x 11.3
312.3+10.5	NGC 5307	18.8 x 12.9
312.6-01.8	He 2-107	10.7 x 8.3
315.0-00.3	He 2-111	29.4 x 14.5
315.1-13.0	He 2-131	10.0 x 9.6
315.4+05.2	He 2-109	11.0 x 7.5
315.4+09.4	He 2-104	85.6 x 34.4
315.7+05.5	LoTr 8	28.4 x 25.1
316.1+08.4	He 2-108	13.6 x 12.3
317.1-05.7	He 2-119	63.3 x 60.4
318.3-02.0	He 2-114	26.1 x 21.4
318.3-02.5	He 2-116	47.9 x 46.7
319.2+06.8	He 2-112	6.9 x 6.3
319.6+15.7	IC 4406	46.4 x 29.9
320.1-09.6	He 2-138	6.7 x 6.0
320.3-28.8	He 2-434	7.4 x 5.1
320.9+02.0	He 2-117	5.4 x 4.4
321.3+02.8	He 2-115	3.4 x 2.4
321.3-16.7	He 2-185	2.9 x 2.5
321.8+01.9	He 2-120	36.1 x 26.5
322.1-06.6	He 2-136	7.3 x 4.8
322.4-00.1	Pe 2- 8	2.5
322.4-02.6	Mz 1	49.3 x 35.3
322.5-05.2	NGC 5979	20.2 x 19.1
323.1-02.5	He 2-132	20.8 x 18.9
323.9+02.4	He 2-123	6.9 x 6.6
324.2+02.5	He 2-125	3.8 x 2.9
324.8-01.1	He 2-133	1.8
325.0+03.2	He 2-129	2.9
325.4-04.0	He 2-141	13.0 x 10.8
325.8+04.5	He 2-128	1.7 :
325.8-12.8	He 2-182	3.1 x 2.8

Table 2. continued.

(1)	(2)	(3)
326.0-06.5	He 2-151	1.8 x 1.7
327.1-01.8	He 2-140	4.1
327.1-02.2	He 2-142	4.2 x 3.1
327.5+13.3	He 2-118	1.3
327.8+10.0	NGC 5882	15.6 x 12.9
327.8-01.6	He 2-143	3.7
327.8-06.1	He 2-158	2.0
327.8-07.2	He 2-163	22.1 x 21.8
327.9-04.3	He 2-147	4.8 x 3.7
328.2+01.3	Lo 10	28.1 x 25.2
328.9-02.4	He 2-146	38.4 x 30.5
330.6-02.1	He 2-153	18.9 x 13.1
330.6-03.6	He 2-159	15.2 x 10.5
330.7+04.1	Cn 1-1	stellar
331.3+16.8	NGC 5873	7.1 x 5.1
331.4+00.5	He 2-145	16.8 x 15.5
331.5-02.7	He 2-161	16.3 x 9.7
331.5-03.9	He 2-165	56.4 x 46.3
331.7-01.0	Mz 3	47.8 x 22.6
332.0-03.3	He 2-164	16.4 x 15.3
332.3-04.2	He 2-170	1.3
332.9-09.9	He 3-1333	3.2 x 2.8
333.4+01.1	He 2-152	11.8 x 10.0
334.3-09.3	IC 4642	24.1 x 21.7
334.8-07.4	SaSt 2-12	15.9 x 11.9
335.4+09.2	ESO 330-02	30.8 x 28.8
335.4-01.1	He 2-169	22.3 x 18.5
336.2+01.9	Pe 1- 6	10.2 x 8.7
336.2-06.9	PC 14	7.2 x 5.1
336.3-05.6	He 2-186	2.9 x 1.4
336.8-07.2	K 2-17	39.3 x 32.4
337.4+01.6	Pe 1- 7	2.4
338.1-08.3	NGC 6326	20.6 x 13.7
338.8+05.6	He 2-155	16.9 x 14.5
340.8+10.8	Lo 12	84.5 x 70.4
340.8+12.3	Lo 11	65.7 x 57.0
341.6+13.7	NGC 6026	53.0 x 45.5
341.8+05.4	NGC 6153	28.0 x 24.2
342.1+10.8	NGC 6072	74.3 x 65.1
342.1+27.5	Me 2-1	8.9 x 8.6
342.9-02.0	Pe 1- 8	24.3 x 22.0
342.9-04.9	He 2-207	37.7 x 26.0
343.4+11.9	H 1- 1	3.1 x 2.7
343.6+03.7	SuWt 3	31.9 x 16.3
345.2-01.2	H 1- 7	10.6 x 8.7
345.2-08.8	Tc 1	12.9 x 12.2
345.4+00.1	IC 4637	18.9 x 13.5
346.2-08.2	IC 4663	20.1 x 14.6
348.0-13.8	IC 4699	12.6 x 8.0
349.3-01.1	NGC 6337	47.6 x 46.5
349.5+01.0	NGC 6302	89.9 x 34.8
350.9+04.4	H 2- 1	4.3 x 3.7
352.9+11.4	K 2-16	26.6 x 24.3
355.1-06.9	M 3-21	2.8
355.4-04.0	Hf 2-1	17.7 x 14.6
356.5-02.3	M 1-27	6.7 x 6.4
356.7-06.4	H 1-51	17.7 x 15.2
357.0+02.4	M 4- 4	6.3 x 5.1
357.1-04.7	H 1-43	2.0
357.3+04.0	H 2- 7	5.7 x 4.4

Table 2. continued.

(1)	(2)	(3)
357.6-03.3	H 2-29	10.7 x 9.8
357.9-03.8	H 2-30	13.3 x 13.3
358.3-21.6	IC 1297	10.8 x 9.8
358.5+05.4	M 3-39	25.9 x 18.1
358.5-07.3	NGC 6563	59.1 x 43.1
358.6+01.8	M 4- 6	2.5 x 2.3
358.6-05.5	M 3-51	20.9 x 14.5
358.9-00.7	M 1-26	6.4 x 6.0
359.0-04.1	M 3-48	5.4 x 4.4
359.1+15.1	A 40	34.3 x 30.4
359.2+01.2	19W32	23.6 x 5.5
359.3-00.9	Hb 5	51.7 x 18.1
359.4-03.4	H 2-33	7.8 x 7.4
359.9+05.1	M 3- 9	17.2 x 15.1

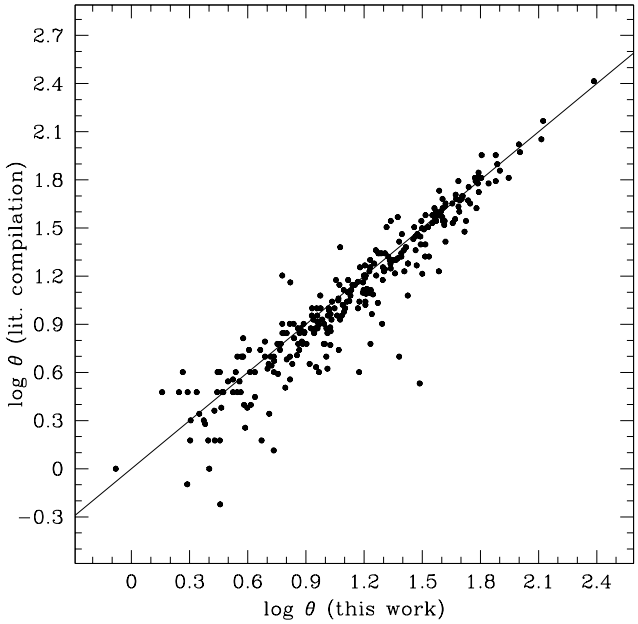

Fig. 9. Comparison of the PN diameters from the literature compilation (see text) with the diameters from this work (geometric means from the two dimensions given in Table 2). Solid line: 1 to 1 relation.

the case of larger nebulae usually concern bipolar nebulae having a compact core, e.g. IC 4634 (000.3+12.2), M 3-28 (021.8–00.4), M 2-48 (062.4–00.2), He 2-104 (315.4+09.4), Hb 5 (359.3–00.9). The published diameters from VLA or optical measurements apparently referred to the core whereas the 10% contour from our images encompassed a significant portion of the outer bipolar structures.

In Fig. 10 we have compared the diameters from Table 2 with the results of VLA surveys of Aaquist & Kwok (1990) and Zijlstra et al. (1989). Aaquist & Kwok observed mainly compact PNe. They have applied three methods for deriving the PN diameters but it is not clear which method(s) has been used to measure a particular object. As can be seen from Fig. 10, our diameters are systematically larger than those of Aaquist & Kwok, on average by factor 1.7. The agreement of our results with those of Zijlstra et al. is better especially if

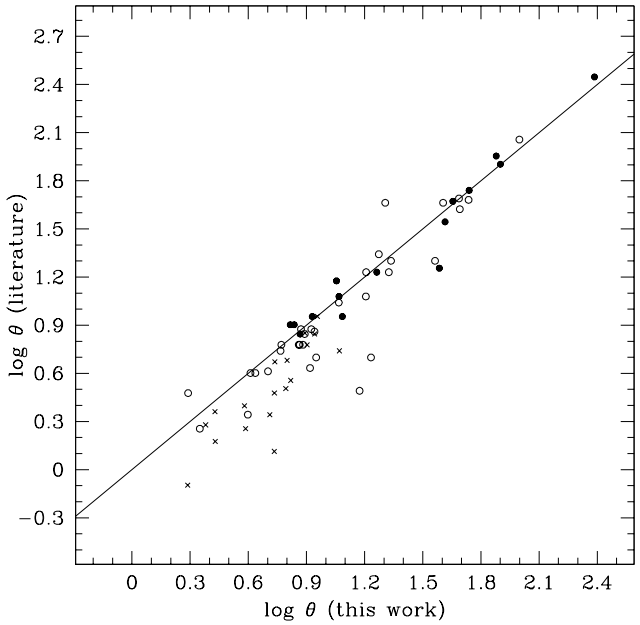

Fig. 10. Comparison of the PN diameters from Aaquist & Kwok (1990) (crosses) and Zijlstra et al. (1989) (full circles – from 10% contour, open circles – from Gaussian deconvolution) with the diameters from this work (geometric means from the two dimensions given in Table 2). Solid line: 1 to 1 relation.

nebulae greater than ∼10 arcsec are considered and the diameter of Zijlstra et al. resulted from their 10% contour (full circles in the figure). In four cases the discrepancy is larger than factor 2. All the cases concern bipolar nebulae. For three of them, i.e already mentioned M 3-28, M 2-48, as well as NGC 2440 (234.8+02.4), our diameters are larger and the reason has been explained above. In the case of M 2-9 our diameter is significantly smaller and it seems that Zijlstra et al. measured the angular extend of the elongated, bipolar lobes whereas our value is a geometric mean from the major and minor axis measurements.

7. Discussion and conclusions

We have measured angular dimensions for 312 PNe. As a primary definition of the PN size we have adopted the extension of nebular emission up to the 10% level of the maximum surface brightness. This seems to be a reasonable choice for extended, well resolved nebulae. For partly resolved objects deconvolution methods have to be used. So far the Gaussian deconvolution has primarily been applied.

We have, however, found that for compact nebulae the 10% contour measurements can also give satisfactory results provided that they are corrected for the finite resolution using Eq. (2). As has been shown in Sects. 5.2 and 5.4 this simple deconvolution of the 10% contour measurments makes the resulting diameters reliable down to nebulae as compact as $\log \Theta_{10\%,d}/\Phi_b \simeq 0.3$ (or equivalently $\log \Phi_d(\mathrm{Gauss})/\Phi_b \simeq 0.05$). The derivation of $\Theta_{10\%,d}$ has several advantages over the deconvolution methods. It is simpler to apply. No assumption has to be made about the surface brightness distribution. It is a more universal method as it can

be applied to compact and partially resolved PNe as well as to extended and well resolved nebulae where the deconvolution methods usually fail in practice.

The Gaussian deconvolution gives fairly reliable and stable results for partly resolved nebulae. However it systematically underestimates the diameters compared to the 10% contour measurements. The difference depends on the model nebula adopted in the Gaussian deconvolution. It is only 5–7% for the constant emissivity sphere but increases up to 45% for a thin shell. This result means that in catalogues and data bases the dimensions of compact PNe, usually derived from the Gaussian deconvolution, are probably underestimated compared to those of extended nebulae. It is difficult to estimate this systematic difference. The deconvolution procedures used in observational surveys, like in Aaquist & Kwok (1990) or Zijlstra et al. (1989), were significantly simplified compared to that of van Hoof (2000). Usually the same value of the conversion factor has been used for all the objects. This certainly introduced additional uncertainties in the final results.

The second-moment deconvolution appeared to give results often uncertain and in poor agreement with the results from the other two methods, in particular for compact nebulae.

Our study does not solve definitevely the problem of measuring the PN dimensions. It makes however an important step in the field in the sense that it gives a quantity which means physically the same and is comparable for all the objects in our sample. One has, however, to remember that the (faint) nebular emission can extend well beyond the diameters given in Table 2. This can be seen for many objects in our sample by comparing Cols. (9) and (8) in Table 1.

Acknowledgements. We are very grateful to the referee (J.J. Condon) whose comments resulted in a significant improvement of the work reported in this paper. This work has partly been supported from a grant No. 2.P03D.020.17 financed by the Polish State Committee for Scientific Research.

References

Aaquist, O. B., & Kwok, S. 1990, A&AS, 84, 229
Acker, A., Ochsenbein, F., Stenholm, B., et al. 1992, Strasbourg-ESO Catalogue of Galactic Planetary Nebulae (ESO publication)
Górny, S. K., Schwarz, H. E., Corradi, R. L. M., & van Winckel, H. 1999, A&AS, 136, 145
Manchado, A., Guerrero, M. A., Stanghellini, L., & Serra-Ricart, M. 1996, The IAC Morphological Catalog of Northern Galactic Planetary Nebulae, Instituto de Astrofisica de Canarias
Schwarz, H. E., Corradi, R. L. M., & Melnick, J. 1992, A&AS, 96, 23
Siódmiak, N., & Tylenda, R. 2001, A&AS, 373, 1032
van Hoof, P. A. M. 2000, MNRAS, 314, 99
Zijlstra, A. A., Pottasch, S. R., & Bignell, C. 1989, A&AS, 79, 329

Online Material

Table 1. Results of measurements (see text for explanation of the columns).

PN G	Main Name	figure	$\Phi_{d,G}$	$\Phi_{b,G}$	$\Phi_{d,sm}$	$\Phi_{b,sm}$	10% level	3σ level	$\%3\sigma$
1	2	3	4	5	6	7	8	9	10
000.1+17.2	PC 12	s 40	1.4 x 1.3	0.8 x 0.7	2.0 x 1.5	0.8 x 0.8	2.7 x 2.6		
000.1-01.1	M 3-43	s 56	2.2 x 1.5	1.4 x 1.5	2.2 x 1.5	1.3 x 1.6	4.8 x 3.7		
000.1-05.6	H 2-40	s 61		1.7 x 1.5	8.9 x 8.5	1.8 x 1.6	18.5 x 17.2		
000.2-01.9	M 2-19	g 28	5.4 x 4.5	1.9 x 1.7	5.1 x 6.0	1.8 x 1.7	10.0 x 9.0	19.0 x 12.7	1.5
000.3+12.2	IC 4634	s 42		0.8 x 0.8		0.8 x 0.8	20.6 x 6.8	24.0 x 19.0	0.3
000.4-01.9	M 2-20	s 56	2.0 x 1.9	1.4 x 1.2	2.8 x 2.5	1.3 x 1.1	4.7 x 4.2		
000.7+04.7	H 2-11	s 49	1.3 x 1.1	1.0 x 1.2	1.5 x 1.3	1.0 x 1.2	2.9 x 2.6		
001.0+01.9	K 1- 4	s 52		1.9 x 1.4		1.4 x 1.3	48.2 x 33.8		
001.5-06.7	SwSt 1	s 66	3.3 x 3.1	1.1 x 1.3	3.9 x 4.1	1.3 x 1.4	6.0 x 5.7		
002.0-13.4	IC 4776	s 74	4.1 x 3.2	1.2 x 1.3	4.5 x 3.1	1.3 x 1.4	8.8 x 4.7	22.1 x 18.2	0.1
002.2-06.3	H 1-63	s 66	2.1 x 1.7	1.7 x 1.5	2.5 x 2.2	1.7 x 1.6	4.9 x 4.2		
002.2-09.4	Cn 1-5	s 69	4.6 x 4.3	0.7 x 0.8	4.2 x 4.0	0.9 x 0.9	7.5 x 7.5	29.9 x 27.6	0.1
002.4+05.8	NGC 6369	s 49		1.5 x 1.2		1.2 x 1.0	33.1 x 32.8	64.7 x 41.4	0.9
002.5-01.7	Pe 2-11	s 58		1.5 x 1.4	3.9 x 3.4	1.6 x 1.5	8.3 x 7.0		
002.7-04.8	M 1-42	s 63		1.4 x 1.6	7.2 x 6.8	1.4 x 1.6	13.3 x 11.7		
002.7-52.4	IC 5148-50	g 9					132.5 x 127.8		
002.8+01.7	H 2-20	s 53	st.	2.1 x 1.8	1.6 x 1.4	1.7 x 1.5	3.9 x 3.1		
003.1+02.9	Hb 4	s 52	5.8 x 4.7	1.5 x 1.6	5.9 x 4.1	1.4 x 1.4	11.4 x 7.4		
003.1+03.4	H 2-17	s 51	2.6 x 2.3	1.5 x 1.4	2.4 x 2.2	1.7 x 1.4	5.5 x 4.7		
003.5-02.4	IC 4673	s 60		0.9 x 0.9	10.7 x 8.3	1.1 x 1.1	22.1 x 15.3		
003.5-04.6	NGC 6565	s 63		1.7 x 1.6	6.5 x 6.2	1.7 x 1.5	11.2 x 10.9		
003.6-02.3	M 2-26	s 59	10.2 x 6.1	1.1 x 1.1	6.0 x 5.3	1.1 x 1.1	10.7 x 10.6		
003.7+07.9	H 2- 8	s 47	3.6 x 3.0	0.8 x 0.9	8.2 x 3.5	0.9 x 0.9	12.0 x 6.9		
003.8-04.5	H 2-41	s 64		1.4 x 1.5	5.1 x 4.6	1.4 x 1.5	9.7 x 9.6		
003.8-17.1	Hb 8	s 76	0.6 x 0.4	1.4 x 1.4	1.5 x 1.3	1.3 x 1.3	2.9 x 2.3		
003.9-14.9	Hb 7	g 13	1.7 x 1.7	1.7 x 1.9	3.0 x 2.8	1.7 x 1.8	4.3 x 4.3		
		s 74	2.2 x 1.8	1.3 x 1.2	4.1 x 2.4	1.4 x 1.3	5.5 x 4.2		
004.0-11.1	M 3-29	s 72	5.6 x 5.4	1.3 x 1.2	4.7 x 5.2	1.4 x 1.3	9.9 x 8.9	15.1 x 12.2	1.4
004.8-22.7	He 2-436	g 24	1.8 x 1.7	1.5 x 1.0	2.1 x 2.0	1.5 x 1.2	4.0 x 4.0		
004.9-04.9	M 1-44	s 66	4.0 x 3.6	1.3 x 1.5	5.2 x 4.4	1.3 x 1.5	6.5 x 6.0	19.9 x 12.2	0.5
005.0+03.0	Pe 1- 9	s 53		1.9 x 1.8	6.8 x 6.7	1.8 x 1.7	14.0 x 13.8		
005.0-03.9	H 2-42	s 64		1.4 x 1.5	6.3 x 6.2	1.4 x 1.6	13.3 x 12.2		
005.1-08.9	Hf 2-2	s 69		1.0 x 1.0	11.6 x 11.3	1.1 x 1.1	21.8 x 21.8		
006.0+03.1	M 1-28	g 1		1.6 x 1.6		1.9 x 1.7	33.2 x 30.4	64.8 x 41.0	4.2
006.1+08.3	M 1-20	s 49	1.3 x 1.3	0.8 x 1.0	1.5 x 1.4	0.9 x 1.0	2.9 x 2.9		
006.8-08.6	Al 1	s 71		1.7 x 1.5	7.7 x 6.4	1.8 x 1.6	15.2 x 12.7		
007.2+01.8	Hb 6	s 57	4.5 x 4.4	1.2 x 1.4	4.1 x 3.8	1.3 x 1.6	8.0 x 7.3		
008.0+03.9	NGC 6445	s 55		1.1 x 1.0		1.2 x 1.1	45.3 x 36.2	188.0 x 116.7	0.5
008.3-01.1	M 1-40	s 62	4.8 x 3.8	1.8 x 1.6	5.3 x 6.0	1.7 x 1.6	9.7 x 8.1	20.8 x 16.4	0.5
008.3-07.3	NGC 6644	s 70	2.4 x 2.3	1.6 x 1.5	2.6 x 2.4	1.8 x 1.6	5.2 x 5.2		
009.4-05.0	NGC 6629	s 68		0.7 x 0.9	8.8 x 8.3	0.8 x 0.9	16.6 x 15.6	40.0 x 38.2	0.5
009.4-09.8	M 3-32	g 29	4.5 x 3.4	2.2 x 2.3	4.2 x 3.5	2.1 x 2.0	9.0 x 8.0		
009.6+10.5	A 41	s 50		1.5 x 1.3	10.5 x 10.4	1.6 x 1.5	20.3 x 17.5		
009.6+14.8	NGC 6309	s 46		0.9 x 1.2	12.5 x 8.4	0.9 x 1.2	22.9 x 12.6	52.3 x 26.5	0.7
009.6-10.6	M 3-33	g 29	4.4 x 3.8	1.7 x 1.6	4.3 x 3.9	1.5 x 1.4	8.0 x 7.9		
010.7-06.4	IC 4732	s 71	1.0 x 0.9	1.8 x 1.9	1.8 x 1.7	1.7 x 1.9	3.6 x 3.4		
010.8+18.0	M 2- 9	s 44		1.2 x 0.9		1.2 x 0.9	37.0 x 11.2	56.0 x 14.8	0.7
010.8-01.8	NGC 6578	s 67	7.1 x 6.8	1.8 x 1.7	6.3 x 6.2	1.9 x 1.7	12.5 x 12.2		
011.0-05.1	M 1-47	g 27	3.3 x 2.9	1.5 x 2.1	3.8 x 3.3	1.5 x 1.9	6.8 x 6.5		
011.1+11.5	M 2-13	s 48	1.5 x 1.4	0.9 x 0.9	2.3 x 1.7	1.0 x 1.0	3.4 x 2.9		
011.7-00.6	NGC 6567	s 65	4.8 x 3.9	1.6 x 1.5	4.7 x 3.6	1.8 x 1.6	8.6 x 7.0		
011.9+04.2	M 1-32	s 57	5.1 x 2.2	1.4 x 1.2	5.1 x 5.0	1.4 x 1.2	9.4 x 8.3	18.3 x 17.4	0.2
012.5-09.8	M 1-62	g 27	2.6 x 2.5	1.9 x 1.8	2.9 x 2.8	1.9 x 1.8	5.8 x 5.8		
013.0-04.3	Pe 2-14	g 34	2.8 x 2.7	2.1 x 1.5	2.6 x 2.9	1.8 x 1.5	6.5 x 6.1		
013.3+32.7	Sn 1	s 38	3.0 x 2.8	1.6 x 1.5	3.5 x 3.0	1.4 x 1.4	6.6 x 5.7		
014.6-04.3	M 1-50	s 70	2.1 x 2.1	1.7 x 1.6	2.4 x 2.3	1.7 x 1.6	5.2 x 4.9		
016.4-01.9	M 1-46	s 68		1.7 x 1.7	6.7 x 6.2	1.5 x 1.4	12.5 x 11.7		

Table 1. continued.

1	2	3	4	5	6	7	8	9	10
017.6-10.2	A 51	s 75		1.4 x 1.3		1.4 x 1.4	59.3 x 59.0		
017.9-04.8	M 3-30	s 73		1.0 x 1.0		1.1 x 1.1	19.2 x 18.5		
020.9-01.1	M 1-51	g 9	7.2 x 6.2	1.8 x 2.1	8.4 x 5.1	2.1 x 2.5	15.9 x 8.9		
021.2-03.9	We 1-7	s 73		1.1 x 1.1		1.2 x 1.1	20.6 x 19.8		
021.7-00.6	M 3-55	s 70	6.4 x 5.8	1.7 x 1.8	6.3 x 5.2	1.7 x 1.7	12.6 x 9.8		
021.8-00.4	M 3-28		9.0 x 6.7	1.9 x 1.8	10.7 x 6.5	2.0 x 2.0	20.9 x 12.3	33.2 x 15.5	2.8
			8.1 x 6.3	1.0 x 1.2	8.2 x 5.2	1.2 x 1.3	27.6 x 12.6		
023.9-02.3	M 1-59		3.6 x 3.5	1.5 x 1.8	5.5 x 3.9	1.6 x 1.8	7.2 x 6.8	24.1 x 16.5	0.2
024.2+05.9	M 4- 9			1.5 x 1.1		1.5 x 1.2	47.9 x 42.0		
		s 65		1.8 x 1.7		1.8 x 1.7	48.1 x 43.4		
024.3-03.3	Pe 1-17		6.0 x 3.6	1.2 x 1.2	7.8 x 4.0	1.5 x 1.5	14.9 x 7.9		
025.8-17.9	NGC 6818	s 84		0.9 x 0.8	13.9 x 12.9	1.0 x 1.0	24.7 x 24.7	35.1 x 32.2	0.4
025.9-10.9	Na 2	s 80	3.9 x 3.3	0.8 x 0.9	3.2 x 3.7	0.9 x 1.1	6.5 x 5.9		
027.3-03.4	A 49	s 74		1.0 x 0.8		0.9 x 0.9	54.1 x 38.2		
027.7+00.7	M 2-45	s 72	5.4 x 5.2	1.2 x 1.1	4.5 x 3.9	1.2 x 1.2	9.6 x 7.8		
028.0+10.2	WeSb 3	s 61		1.7 x 1.7		1.5 x 1.4	50.8 x 43.2		
028.7-03.9	Pe 1-21			1.7 x 1.1	5.6 x 4.9	1.6 x 1.2	11.5 x 10.6		
029.2-05.9	NGC 6751	s 76		1.1 x 1.1	15.9 x 14.1	1.3 x 1.3	24.2 x 23.3	55.4 x 54.1	0.6
030.8+03.4	A 47	s 72		1.5 x 1.3		1.3 x 1.1	17.7 x 12.6		
031.0-10.8	M 3-34	s 82	4.3 x 3.8	0.9 x 1.0	4.0 x 3.3	1.0 x 1.1	7.6 x 6.6	10.7 x 9.3	0.6
033.0-05.3	A 55	s 77		1.7 x 1.6		1.7 x 1.6	56.9 x 52.4		
033.1-06.3	NGC 6772	s 79		1.8 x 1.6		1.6 x 1.5	80.8 x 70.9		
033.8-02.6	NGC 6741	s 75	5.3 x 4.4	1.3 x 1.4	5.2 x 3.8	1.3 x 1.3	9.4 x 7.0		
034.5-06.7	NGC 6778	s 80		1.1 x 0.9	13.2 x 10.9	1.0 x 0.9	21.5 x 15.6	39.5 x 31.0	0.6
035.9-01.1	Sh 2- 71			1.3 x 1.1		1.5 x 1.4	132.4 x 74.9	168.4 x 85.1	5.1
037.5-05.1	A 58	s 80		1.1 x 1.0		1.1 x 1.0	44.7 x 33.7		
037.7-34.5	NGC 7009	s 85		1.4 x 1.0	14.3 x 11.4	1.0 x 0.7	28.1 x 22.1	55.0 x 29.6	0.6
037.8-06.3	NGC 6790	s 81	2.5 x 2.1	0.9 x 0.7	2.7 x 2.5	0.9 x 0.7	4.7 x 3.6		
038.1-25.4	A 70	s 85		1.2 x 1.2		1.4 x 1.3	45.2 x 37.9		
038.2+12.0	Cn 3-1	s 67	3.3 x 3.2	0.9 x 1.1	3.1 x 3.2	0.9 x 0.9	6.0 x 4.9		
039.5-02.7	M 2-47	s 78	4.0 x 2.8	1.6 x 1.9	3.8 x 3.1	1.5 x 1.8	7.5 x 6.0		
040.3-00.4	A 53	s 76		1.1 x 1.2	19.3 x 18.8	1.1 x 1.1	32.0 x 31.2		
042.9-06.9	NGC 6807	s 83	1.3 x 1.3	1.0 x 0.9	1.6 x 1.6	1.1 x 1.1	2.6 x 2.6		
043.1+03.8	M 1-65	s 75	2.3 x 2.3	1.2 x 1.4	2.6 x 2.5	1.1 x 1.3	4.7 x 4.7	12.0 x 12.2	0.3
043.3+11.6	M 3-27	s 69	1.4 x 1.2	1.1 x 1.2	1.8 x 1.8	1.3 x 1.3	3.5 x 3.1		
045.4-02.7	Vy 2-2	s 81	1.6 x 1.5	0.9 x 1.0	2.1 x 1.9	0.8 x 0.9	3.6 x 3.1	13.0 x 12.5	0.1
045.7-04.5	NGC 6804	s 83		1.3 x 1.1		1.4 x 1.2	58.3 x 48.6		
046.4-04.1	NGC 6803	s 83	3.2 x 2.7	1.0 x 1.2	3.2 x 2.9	1.1 x 1.3	5.7 x 5.5		
054.1-12.1	NGC 6891		7.6 x 6.4	2.0 x 1.6	7.4 x 6.8	2.2 x 1.9	14.0 x 13.0		
061.4-09.5	NGC 6905			2.6 x 2.3		2.6 x 2.3	43.5 x 35.9		
062.4-00.2	M 2-48		9.3 x 5.7	2.6 x 2.8	10.5 x 6.4	2.3 x 2.4	20.0 x 12.4	29.0 x 15.6	4.5
065.2-05.6	He 1- 6			2.3 x 2.2		2.5 x 2.5	40.7 x 21.9		
066.7-28.2	NGC 7094			1.5 x 1.3		1.6 x 1.5	102.5 x 99.4		
069.2+03.8	K 3-46			2.2 x 2.3	21.4 x 9.7	2.4 x 2.5	36.4 x 23.9		
069.4-02.6	NGC 6894			2.4 x 2.3		2.4 x 2.4	56.6 x 53.5		
118.8-74.7	NGC 246	g 30					260.4 x 226.7		
161.2-14.8	IC 2003		6.1 x 4.8	2.3 x 2.6	5.6 x 4.7	2.2 x 2.6	10.8 x 9.4		
171.3-25.8	Ba 1			2.1 x 2.0		1.9 x 1.9	40.0 x 38.5		
174.2-14.6	H 3-29		9.7 x 9.2	2.5 x 2.2	7.8 x 5.6	2.5 x 2.3	24.2 x 19.2		
189.1+19.8	NGC 2371-72						48.9 x 30.6	130.9 x 55.7	1.9
190.3-17.7	J 320	s 1	5.8 x 2.8	2.0 x 2.1	5.3 x 3.8	1.9 x 1.8	10.1 x 7.4	22.4 x 12.6	0.7
194.2+02.5	J 900	s 5	4.6 x 4.2	2.0 x 1.7	4.5 x 4.7	1.8 x 1.6	8.8 x 8.6		
196.6-10.9	NGC 2022	s 2		1.5 x 1.4	14.5 x 13.6	1.3 x 1.3	28.0 x 25.6	32.0 x 30.7	2.6
197.2-14.2	K 1- 7	s 2		1.4 x 1.4	19.6 x 17.6	1.3 x 1.3	37.3 x 36.1		
198.6-06.3	A 12	s 3		1.3 x 1.2	23.1 x 22.8	1.3 x 1.2	44.2 x 38.6		
201.9-04.6	We 1-4	s 4		0.9 x 0.9		1.0 x 1.0	41.4 x 37.6		
206.4-40.5	NGC 1535	s 1					33.3 x 32.1	51.5 x 49.1	0.5
212.0+04.3	M 1- 9		1.5 x 1.4	2.2 x 1.8	2.1 x 2.0	2.1 x 1.8	4.7 x 4.3		
214.9+07.8	A 20	s 8		2.2 x 2.0		2.2 x 2.1	67.4 x 60.6		

Table 1. continued.

1	2	3	4	5	6	7	8	9	10
216.3-04.4	We 1-5	s 5		1.9 x 1.7		1.6 x 1.5	20.6 x 19.5		
221.3-12.3	IC 2165	s 4	5.8 x 5.0	2.2 x 2.1	5.4 x 5.0	1.9 x 1.8	10.1 x 9.7		
221.7+05.3	M 3- 3			2.0 x 2.2	9.3 x 8.3	2.0 x 2.2	17.1 x 16.2		
224.9+01.0	We 1-6	s 8		2.1 x 2.0		1.9 x 1.8	61.0 x 58.5		
226.4-03.7	PB 1	g 32	5.8 x 5.5	1.9 x 2.3	4.9 x 4.8	1.9 x 2.3	11.2 x 10.4		
226.7+05.6	M 1-16	s 9	3.9 x 3.1	2.4 x 2.3	5.3 x 4.0	2.3 x 2.2	8.8 x 7.0	96.6 x 19.6	0.1
228.8+05.3	M 1-17	g 27	2.1 x 1.8	2.3 x 2.1	2.7 x 2.4	2.1 x 1.9	5.8 x 5.4		
229.6-02.7	K 1-10	s 8		1.0 x 0.8		1.3 x 1.1	51.3 x 46.0	90.5 x 60.4	3.6
231.4+04.3	M 1-18	s 10		1.5 x 1.7	19.1 x 18.3	1.6 x 1.9	35.0 x 33.0		
231.8+04.1	NGC 2438	s 9		1.1 x 1.0		1.5 x 1.4	80.7 x 78.3		
232.4-01.8	M 1-13	g 26		1.5 x 1.7	9.5 x 6.9	2.1 x 2.2	18.8 x 12.0		
232.8-04.7	M 1-11	s 7	3.2 x 2.9	1.1 x 1.0		1.3 x 1.2	5.5 x 5.5		
233.5-16.3	A 15	s 5		2.1 x 1.8		1.5 x 1.3	36.7 x 34.9		
234.8+02.4	NGC 2440	s 10		1.6 x 1.4		1.6 x 1.3	58.9 x 25.3	74.6 x 55.6	0.2
234.9-01.4	M 1-14	g 26	3.3 x 2.6	1.7 x 2.2	3.4 x 3.0	1.7 x 1.9	6.5 x 6.5		
236.7+03.5	K 1-12	s 11		1.5 x 1.4		1.2 x 1.1	44.2 x 36.5		
238.9+07.3	Sa 2-21	s 12		1.2 x 0.9		1.1 x 0.9	40.4 x 34.4		
239.6+13.9	NGC 2610			1.4 x 1.2	25.4 x 23.8	1.4 x 1.4	47.5 x 46.6		
		s 14		0.9 x 0.8		0.9 x 0.8	52.0 x 48.6		
240.3-07.6	M 3- 2	g 1		1.8 x 1.8	7.3 x 5.8	1.9 x 2.0	12.7 x 9.7	34.9 x 15.9	3.0
242.6-11.6	M 3- 1	g 28	7.2 x 4.2	1.7 x 1.7	7.0 x 7.7	2.0 x 1.8	13.1 x 11.6	28.0 x 17.4	1.1
		s 6	7.3 x 5.9	1.9 x 1.8	7.0 x 6.3	1.5 x 1.6	13.0 x 10.9	27.8 x 16.4	2.2
243.3-01.0	NGC 2452	s 10		1.5 x 1.4	12.4 x 10.7	1.7 x 1.4	18.5 x 12.7	33.6 x 27.6	0.7
245.4+01.6	M 3- 5	s 11	5.0 x 4.8	1.0 x 1.2	4.6 x 4.7	0.9 x 1.1	8.6 x 7.5		
248.8-08.5	M 4- 2	s 9	5.1 x 3.7	1.8 x 1.7	4.3 x 3.6	1.7 x 1.7	8.8 x 7.8		
249.0+06.9	SaSt 1- 1	s 13	0.7 x 0.7	0.8 x 0.6	1.1 x 1.1	0.9 x 0.8	1.8 x 1.6	13.5 x 13.0	0.1
250.3+00.1	A 26	g 12		1.3 x 1.3		1.4 x 1.4	37.6 x 36.8		
252.6+04.4	K 1- 1	s 13		0.8 x 0.8		0.8 x 0.8	51.3 x 47.5		
258.1-00.3	He 2- 9	s 13	3.2 x 3.2	0.7 x 0.9	2.9 x 2.8	0.9 x 0.9	6.0 x 5.0		
259.1+00.9	He 2- 11	g 13		1.6 x 1.5		1.5 x 1.2	121.7 x 64.1		
261.0+32.0	NGC 3242	s 19		1.0 x 0.7		0.9 x 0.7	31.5 x 30.7	62.9 x 54.6	0.1
261.9+08.5	NGC 2818	g 10		1.4 x 1.2		1.7 x 1.7	56.2 x 46.1	118.1 x 56.5	2.1
262.6-04.6	Wray 17-18	s 12		0.9 x 0.8		0.9 x 0.9	17.3 x 16.9		
264.4-12.7	He 2- 5	s 11	2.0 x 1.8	1.4 x 1.3	2.2 x 2.0	1.4 x 1.2	4.4 x 4.4		
265.7+04.1	NGC 2792	s 15		0.7 x 0.7	9.7 x 9.0	0.7 x 0.7	17.9 x 16.4	25.0 x 22.1	1.1
268.4+02.4	PB 5	s 15	1.0 x 1.0	0.7 x 0.7	1.2 x 1.0	0.7 x 0.8	2.1 x 2.1		
272.1+12.3	NGC 3132	s 18		0.8 x 0.8		0.8 x 0.7	59.9 x 45.6	86.7 x 58.5	0.4
273.2-03.7	He 2- 18	g 14	9.3 x 7.3	2.1 x 1.8	6.9 x 7.3	2.3 x 2.1	16.7 x 14.2		
274.3+09.1	Lo 4	s 17		0.7 x 0.7		0.7 x 0.7	41.6 x 38.9		
274.6+02.1	He 2- 35	g 15	2.2 x 2.0	2.0 x 1.7	2.4 x 2.3	2.0 x 1.7	5.4 x 4.7		
274.6+03.5	He 2- 37	g 15		1.8 x 1.9	13.3 x 13.0	2.1 x 2.2	26.3 x 22.4		
275.0-04.1	PB 4	s 15		0.8 x 0.8	6.9 x 5.3	0.9 x 0.9	12.3 x 10.3	18.2 x 13.0	1.3
275.2-02.9	He 2- 28	g 14	5.9 x 5.9	2.1 x 2.3	5.1 x 4.8	2.5 x 2.6	11.5 x 10.8		
275.2-03.7	He 2- 25	s 16		0.7 x 0.7		0.8 x 0.8	54.2 x 10.7		
275.8-02.9	He 2- 29	g 14	7.8 x 4.5	2.2 x 1.8	8.7 x 7.7	2.4 x 2.1	16.3 x 12.5	19.4 x 15.9	1.9
277.1-03.8	NGC 2899	g 11		1.7 x 1.5		1.9 x 2.0	68.6 x 59.9	117.5 x 66.1	2.1
278.1-05.9	NGC 2867	s 16		0.7 x 0.8	8.6 x 8.3	0.8 x 0.8	14.5 x 14.0	28.3 x 27.3	0.1
279.6-03.1	He 2- 36	s 17		0.8 x 0.7	11.1 x 8.8	0.8 x 0.9	24.8 x 15.3	31.1 x 20.0	0.7
283.8+02.2	My 60	s 19		0.8 x 0.6	5.3 x 5.1	0.8 x 0.7	10.2 x 10.2	13.0 x 12.8	1.0
283.8-04.2	He 2- 39	g 15	8.3 x 7.0	2.1 x 1.8	6.2 x 6.0	2.2 x 1.9	13.0 x 12.6		
283.9-01.8	Hf 4	s 18		0.8 x 0.8		0.8 x 0.8	29.1 x 21.0	40.2 x 29.4	3.8
285.4+02.2	Pe 2- 7	g 33	3.0 x 2.0	1.8 x 2.1	2.7 x 2.1	1.9 x 2.0	6.5 x 5.8		
285.4-05.3	IC 2553	s 18	5.4 x 4.4	0.7 x 0.9	5.7 x 4.1	0.8 x 0.9	11.6 x 7.6	19.5 x 16.6	0.1
285.6-02.7	He 2- 47	g 16	2.7 x 2.6	2.1 x 2.4	3.4 x 3.6	2.0 x 2.3	6.5 x 5.8		
285.7+01.2	Pe 1- 2	s 20	2.0 x 1.9	0.7 x 0.8	2.0 x 3.0	0.8 x 0.8	4.2 x 3.4	15.6 x 7.6	0.2
285.7-14.9	IC 2448	s 14	5.5 x 4.7	0.5 x 0.5	5.5 x 5.4	0.5 x 0.5	10.7 x 10.0		
286.3-04.8	NGC 3211	g 31	9.7 x 7.7	2.4 x 2.6	8.5 x 8.4	2.5 x 2.6	16.7 x 16.6		
288.4-02.4	Pe 1- 3	g 32	5.9 x 5.5	2.0 x 2.3	4.5 x 5.2	2.2 x 2.5	11.5 x 9.8		
289.8+07.7	He 2- 63	g 16	1.7 x 1.4	2.0 x 1.8	1.8 x 1.6	1.9 x 1.8	4.7 x 4.5		

Table 1. continued.

1	2	3	4	5	6	7	8	9	10
291.4+19.2	ESO 320-28	s 22		1.2 x 0.9		1.0 x 0.9	30.4 x 27.3		
291.6-04.8	IC 2621	s 20	2.6 x 2.2	1.0 x 0.9	2.7 x 2.3	1.0 x 0.9	4.4 x 3.9		
291.7+03.7	He 2- 64	s 21	5.6 x 3.5	0.9 x 0.9	6.0 x 7.1	1.0 x 1.0	9.2 x 8.5	21.4 x 11.8	2.4
292.4+04.1	PB 8	s 21	4.1 x 3.7	0.9 x 1.0	3.6 x 3.7	0.9 x 1.0	6.8 x 6.8		
292.6+01.2	NGC 3699	g 11		1.4 x 1.2		1.5 x 1.4	47.0 x 37.1	62.9 x 54.0	3.8
292.8+01.1	He 2- 67	g 2	2.5 x 1.9	1.9 x 1.9	3.8 x 2.6	1.9 x 1.9	6.2 x 4.4	19.4 x 12.8	0.3
293.6+01.2	He 2- 70	g 3		1.3 x 1.2		1.4 x 1.4	34.7 x 13.8	74.6 x 51.9	1.7
294.1+14.4	Lo 6	s 22		1.1 x 1.0		1.1 x 1.0	77.0 x 74.4		
294.6+04.7	NGC 3918	s 22	10.7 x 9.9	1.0 x 1.1	9.1 x 9.3	1.0 x 1.1	18.8 x 17.2	48.5 x 43.7	0.1
294.9-04.3	He 2- 68	g 16	1.3 x 1.3	1.8 x 1.7	2.2 x 2.1	1.8 x 1.7	4.3 x 4.0		
296.3-03.0	He 2- 73	s 21	1.7 x 1.5	1.1 x 1.0	2.1 x 1.7	1.1 x 1.1	3.9 x 3.1		
296.6-20.0	NGC 3195	g 2		1.5 x 1.6	20.4 x 20.2	1.6 x 1.7	39.6 x 33.9		
297.4+03.7	He 2- 78	g 17	1.9 x 1.9	2.4 x 1.9	2.4 x 2.2	2.4 x 2.1	5.4 x 5.0		
298.1-00.7	He 2- 77	g 17	10.0 x 6.6	1.8 x 1.9	14.4 x 8.0	2.2 x 2.2	25.6 x 14.5	47.4 x 32.1	2.4
298.2-01.7	He 2- 76	g 3	6.5 x 4.9	1.8 x 1.9	7.9 x 11.0	2.0 x 2.1	17.4 x 17.3	40.7 x 21.3	4.6
298.3-04.8	NGC 4071	g 31		1.5 x 1.3		1.6 x 1.5	52.7 x 72.4		
299.0+18.4	K 1-23	s 23		1.2 x 1.2		1.1 x 1.0	64.3 x 56.4		
299.5+02.4	He 2- 82	g 4		1.8 x 1.7	15.2 x 14.7	1.7 x 1.9	32.0 x 25.6		
299.8-01.3	He 2- 81	g 17	4.2 x 3.7	1.7 x 1.7	3.7 x 3.4	1.6 x 1.7	7.9 x 7.2		
300.2+00.6	He 2- 83	g 18	2.7 x 2.4	1.9 x 2.0	2.8 x 3.0	1.9 x 1.9	5.8 x 5.8		
300.4-00.9	He 2- 84	g 4		1.4 x 1.1		1.3 x 1.2	35.9 x 23.8		
300.5-01.1	He 2- 85	g 18	5.2 x 3.4	2.0 x 2.1	4.4 x 4.9	2.0 x 2.1	10.0 x 8.7		
300.7-02.0	He 2- 86	g 18	2.0 x 1.2	2.0 x 1.9	3.0 x 1.7	2.1 x 1.9	5.6 x 4.3		
304.5-04.8	IC 4191	s 23	3.3 x 2.9	0.9 x 1.1	3.8 x 3.9	0.9 x 1.1	5.6 x 4.9	23.0 x 20.5	0.1
304.8+05.1	He 2- 88	g 19	0.7 x 0.7	2.6 x 1.7	1.7 x 1.6	2.4 x 1.7	4.7 x 4.0		
305.1+01.4	He 2- 90	s 24	1.7 x 1.6	1.2 x 1.0	2.5 x 2.3	1.2 x 1.1	3.9 x 3.6		
306.4-00.6	Th 2- A	g 34		2.5 x 2.4	15.8 x 13.2	2.7 x 2.6	27.7 x 25.2		
307.2-03.4	NGC 5189	g 11		1.7 x 1.6		2.2 x 1.9	163.4 x 108.2	177.6 x 130.9	2.1
307.2-09.0	He 2- 97	s 25	1.4 x 1.2	1.3 x 1.1	1.6 x 1.5	1.2 x 1.1	3.6 x 2.6		
307.5-04.9	MyCn 18	s 24		1.4 x 1.2		1.4 x 1.3	17.4 x 10.1	23.7 x 17.7	0.5
308.6-12.2	He 2-105	s 27		1.3 x 1.1		1.1 x 1.1	41.6 x 40.7		
309.0+00.8	He 2- 96	g 19	1.5 x 1.3	2.1 x 2.0	2.8 x 2.2	2.1 x 2.1	4.7 x 4.7		
309.0-04.2	He 2- 99	s 25		1.3 x 1.0	13.3 x 12.1	1.3 x 1.1	28.0 x 23.5		
309.1-04.3	NGC 5315	s 25	6.0 x 5.9	1.0 x 1.1	5.7 x 5.9	1.1 x 1.2	10.9 x 9.4	50.7 x 44.0	0.1
310.7-02.9	He 2-103	g 20		1.5 x 1.7	11.4 x 11.0	1.8 x 1.9	22.3 x 21.1		
311.0+02.4	SuWt 2	s 26		1.0 x 0.8		1.0 x 0.9	86.5 x 43.4		
311.4+02.8	He 2-102	g 19	6.5 x 5.6	2.2 x 2.1	5.4 x 5.8	2.5 x 2.5	12.3 x 12.0		
312.3+10.5	NGC 5307	g 31	12.0 x 6.7	2.4 x 2.3	9.7 x 6.7	2.9 x 2.8	19.3 x 13.6		
312.6-01.8	He 2-107	s 28	7.2 x 5.1	1.3 x 1.2	6.0 x 4.7	1.5 x 1.5	11.0 x 8.6		
315.0-00.3	He 2-111	g 20		1.8 x 1.7	20.2 x 12.0	2.2 x 2.1	29.6 x 14.8	106.6 x 52.7	0.5
315.1-13.0	He 2-131	s 33		1.1 x 1.0		1.1 x 1.1	10.2 x 9.8		
315.4+05.2	He 2-109	g 20	5.6 x 5.5	1.9 x 1.8	5.2 x 4.2	2.0 x 2.0	11.5 x 8.2		
315.4+09.4	He 2-104	s 26		1.4 x 1.0		1.3 x 1.1	85.6 x 34.4		
315.7+05.5	LoTr 8	s 28		1.1 x 1.0		1.3 x 1.2	28.5 x 25.2		
316.1+08.4	He 2-108	s 27		1.4 x 1.1	7.3 x 6.8	1.3 x 1.2	13.8 x 12.5		
317.1-05.7	He 2-119	g 5		1.8 x 1.7		1.7 x 1.6	63.4 x 60.5	108.6 x 68.9	2.5
318.3-02.0	He 2-114	g 4		1.7 x 1.8	13.7 x 13.2	1.9 x 1.9	26.3 x 21.6		
318.3-02.5	He 2-116	g 5		3.3 x 2.9	27.3 x 26.2	3.2 x 2.9	48.2 x 47.1		
319.2+06.8	He 2-112	g 21	3.9 x 3.9	1.8 x 1.9	3.8 x 3.7	1.8 x 1.9	7.6 x 7.2		
319.6+15.7	IC 4406	s 28		1.3 x 1.2		1.5 x 1.5	46.5 x 30.0	103.7 x 39.3	0.7
320.1-09.6	He 2-138	g 22	3.9 x 3.7	1.7 x 1.8	4.0 x 3.8	1.6 x 1.8	7.3 x 6.8		
320.3-28.8	He 2-434	s 82	3.5 x 2.4	1.2 x 0.9	3.6 x 2.6	1.0 x 0.8	7.7 x 5.3		
320.9+02.0	He 2-117	s 29	2.9 x 2.9	0.7 x 0.6	3.1 x 2.8	0.7 x 0.7	5.5 x 4.5		
321.3+02.8	He 2-115	g 21	1.8 x 1.5	1.3 x 1.2	2.3 x 2.0	1.3 x 1.2	4.5 x 3.1		
		s 29	1.6 x 1.5	0.7 x 0.7	1.9 x 1.5	0.9 x 0.8	3.4 x 2.4		
321.3-16.7	He 2-185	s 41	1.7 x 1.3	0.8 x 0.7	1.6 x 1.4	0.9 x 0.9	3.3 x 2.8		
321.8+01.9	He 2-120	g 5		1.7 x 1.7	19.7 x 17.0	1.8 x 1.7	36.2 x 26.7		
322.1-06.6	He 2-136	s 34	3.9 x 3.8	1.2 x 1.2	3.3 x 4.2	1.3 x 1.3	7.6 x 5.2		
322.4-00.1	Pe 2- 8	g 33	1.2 x 1.0	2.7 x 2.2	2.2 x 2.0	2.6 x 2.1	5.8 x 4.7		

Table 1. continued.

1	2	3	4	5	6	7	8	9	10
322.4-02.6	Mz 1	s 32		0.9 x 0.9		1.0 x 1.0	49.3 x 35.3		
322.5-05.2	NGC 5979	s 33		1.1 x 1.2	11.5 x 10.5	1.2 x 1.3	20.3 x 19.2	26.6 x 23.3	1.2
323.1-02.5	He 2-132	g 22		1.9 x 1.9	10.8 x 9.9	2.1 x 2.1	21.1 x 19.2		
323.9+02.4	He 2-123	s 31	4.3 x 3.5	0.9 x 0.9	4.1 x 5.9	1.0 x 1.0	7.1 x 6.8	34.4 x 12.2	0.2
324.2+02.5	He 2-125	s 31	2.0 x 1.8	0.9 x 1.0	2.1 x 1.8	1.0 x 1.0	4.2 x 3.4		
324.8-01.1	He 2-133	s 33	1.1 x 1.0	1.0 x 1.1	1.6 x 1.6	1.1 x 1.2	2.9 x 2.3		
325.0+03.2	He 2-129	g 21	1.7 x 1.4	1.8 x 1.7	2.0 x 1.8	1.9 x 1.8	4.3 x 4.3		
325.4-04.0	He 2-141	s 35		0.9 x 1.0	9.9 x 7.3	1.0 x 1.0	13.1 x 10.9	33.3 x 16.0	0.6
325.8+04.5	He 2-128	s 32	1.2 x 1.0	0.9 x 0.9	1.4 x 1.2	0.9 x 1.0	2.3 x 2.1		
325.8-12.8	He 2-182	s 41	1.9 x 1.9	0.7 x 0.8	2.2 x 2.0	0.9 x 0.9	3.4 x 3.1		
326.0-06.5	He 2-151	s 37	1.0 x 0.9	0.8 x 0.8	1.2 x 1.1	0.9 x 0.9	2.3 x 2.3		
327.1-01.8	He 2-140	g 22	2.4 x 2.1	2.5 x 2.0	2.8 x 2.6	2.6 x 2.3	6.2 x 5.4		
327.1-02.2	He 2-142	s 35	2.4 x 2.2	0.9 x 0.8	2.4 x 2.1	0.9 x 0.9	4.4 x 3.5		
327.5+13.3	He 2-118	s 30	1.0 x 0.7	0.7 x 0.7	1.0 x 0.8	0.8 x 0.7	1.8 x 1.6		
327.8+10.0	NGC 5882	s 30		0.7 x 0.7	7.8 x 6.9	0.7 x 0.7	15.6 x 13.0		
327.8-01.6	He 2-143	g 23	2.4 x 1.5	2.4 x 2.4	3.1 x 2.0	2.5 x 2.5	6.5 x 5.1		
327.8-06.1	He 2-158	s 38	1.3 x 0.9	1.3 x 1.4	2.0 x 1.5	1.4 x 1.5	3.4 x 2.9		
327.8-07.2	He 2-163	g 24		1.8 x 1.7	12.8 x 10.8	2.0 x 1.9	22.3 x 22.0		
327.9-04.3	He 2-147	g 23	2.1 x 1.3	1.8 x 1.6	2.4 x 1.6	1.8 x 1.7	5.8 x 4.7		
328.2+01.3	Lo 10	s 34		1.3 x 1.2		1.2 x 1.2	28.2 x 25.3		
328.9-02.4	He 2-146	g 6		1.5 x 1.2		1.7 x 1.6	38.5 x 30.6		
330.6-02.1	He 2-153	g 7		1.8 x 1.6	10.5 x 8.8	2.0 x 2.0	19.1 x 13.5		
330.6-03.6	He 2-159	g 23	6.9 x 5.2	1.6 x 1.4	7.8 x 4.7	1.7 x 1.7	15.5 x 10.8		
330.7+04.1	Cn 1-1	g 12	st.	2.4 x 1.7	1.8 x 1.7	2.4 x 1.8	4.3 x 2.9		
331.3+16.8	NGC 5873	s 30	4.8 x 2.8	0.6 x 0.7	3.4 x 4.0	0.8 x 0.8	7.2 x 5.2	12.8 x 12.2	0.1
331.4+00.5	He 2-145	g 6		1.6 x 1.5	9.8 x 9.5	1.9 x 1.7	17.0 x 15.7	24.5 x 18.3	4.7
331.5-02.7	He 2-161	g 7	6.7 x 4.7	1.7 x 1.8	5.6 x 8.3	1.9 x 1.9	16.6 x 10.2		
331.5-03.9	He 2-165	g 8		1.5 x 1.5	29.7 x 25.5	1.9 x 1.7	56.5 x 46.4		
331.7-01.0	Mz 3	s 37		0.9 x 0.8		0.9 x 0.8	47.8 x 22.6		
332.0-03.3	He 2-164	g 8	10.1 x 8.6	1.5 x 1.4	8.2 x 9.4	1.6 x 1.8	16.6 x 15.5		
332.3-04.2	He 2-170	s 39	0.7 x 0.6	0.8 x 0.9	0.9 x 0.8	0.9 x 0.9	2.1 x 1.8		
332.9-09.9	He 3-1333	s 44	1.8 x 1.6	1.1 x 0.9	2.4 x 2.1	1.2 x 1.1	3.6 x 3.4		
333.4+01.1	He 2-152	g 6	6.1 x 6.1	1.8 x 1.7	7.6 x 6.9	1.9 x 2.0	12.2 x 10.5		
334.3-09.3	IC 4642	s 45		1.2 x 0.9	12.2 x 11.1	1.0 x 1.0	24.2 x 21.8		
334.8-07.4	SaSt 2-12	s 42		0.7 x 0.6		0.8 x 0.7	16.0 x 11.9		
335.4+09.2	ESO 330-02	s 34		1.2 x 1.1		1.2 x 1.2	30.9 x 28.9		
335.4-01.1	He 2-169	g 8		1.7 x 1.6		1.9 x 1.7	22.5 x 18.7	29.6 x 23.4	4.8
336.2+01.9	Pe 1- 6	g 33	6.2 x 4.3	1.7 x 1.5	4.7 x 4.6	1.7 x 1.7	10.6 x 9.2		
336.2-06.9	PC 14	s 43	3.3 x 2.8	0.9 x 0.8	3.0 x 3.9	1.0 x 0.9	7.3 x 5.4		
336.3-05.6	He 2-186	s 41	1.5 x 1.0	0.6 x 0.8	1.8 x 1.7	0.7 x 0.8	3.1 x 2.1	10.7 x 7.3	0.1
336.8-07.2	K 2-17	s 45		1.1 x 0.9		1.3 x 1.1	39.3 x 32.5		
337.4+01.6	Pe 1- 7	s 39	1.4 x 1.2	1.2 x 1.3	2.0 x 2.0	1.3 x 1.3	3.4 x 3.1		
338.1-08.3	NGC 6326	s 46		1.0 x 1.0	11.8 x 9.1	1.2 x 1.3	20.7 x 13.8	38.5 x 23.7	0.7
338.8+05.6	He 2-155	g 7	11.9 x 8.7	1.3 x 1.6	9.2 x 8.5	1.5 x 1.6	17.1 x 14.7	24.2 x 19.5	3.2
340.8+10.8	Lo 12	g 25		1.3 x 1.3		1.6 x 1.5	84.5 x 70.4		
340.8+12.3	Lo 11	s 36		0.9 x 0.8		0.9 x 0.9	65.7 x 57.0		
341.6+13.7	NGC 6026	s 35		0.8 x 0.7		0.8 x 0.8	53.0 x 45.5		
341.8+05.4	NGC 6153	g 32		2.6 x 1.9	15.2 x 14.0	2.6 x 2.2	28.4 x 24.5		
342.1+10.8	NGC 6072	s 36		0.8 x 0.7		0.8 x 0.8	74.3 x 65.1		
342.1+27.5	Me 2-1	s 31	4.9 x 4.9	1.1 x 0.9	4.5 x 4.4	1.1 x 1.0	9.1 x 8.8		
342.9-02.0	Pe 1- 8	g 12		1.8 x 1.0		1.7 x 1.3	24.5 x 22.1		
342.9-04.9	He 2-207	g 24		1.6 x 1.4		1.8 x 1.7	37.8 x 26.1		
343.4+11.9	H 1- 1	s 36	1.6 x 1.4	0.8 x 0.8	1.6 x 1.5	0.9 x 0.9	3.4 x 3.1		
343.6+03.7	SuWt 3	s 39		0.8 x 0.8		0.9 x 0.8	31.9 x 16.4		
345.2-01.2	H 1- 7	s 45	5.7 x 5.2	1.0 x 0.7	5.2 x 6.0	1.0 x 0.9	10.7 x 8.9		
345.2-08.8	Tc 1	s 53	8.1 x 7.1	1.9 x 1.6	6.8 x 6.4	1.7 x 1.5	13.3 x 12.5	52.0 x 51.0	0.4
345.4+00.1	IC 4637	s 43		0.8 x 0.8	11.4 x 10.0	0.9 x 0.9	19.0 x 13.6	30.2 x 25.5	0.5
346.2-08.2	IC 4663	s 52		1.6 x 1.7	10.4 x 8.7	1.6 x 1.7	20.3 x 14.9		
348.0-13.8	IC 4699	s 67	8.4 x 3.5	1.7 x 1.8	7.0 x 3.9	1.7 x 1.8	13.0 x 8.7		

Table 1. continued.

1	2	3	4	5	6	7	8	9	10
349.3-01.1	NGC 6337	s 47		1.0 x 0.9		1.1 x 1.0	47.6 x 46.5		
349.5+01.0	NGC 6302	s 46		0.8 x 0.7		0.9 x 0.8	89.9 x 34.8		
350.9+04.4	H 2- 1	s 42	2.3 x 2.2	0.8 x 0.7	2.5 x 2.5	0.9 x 0.8	4.5 x 3.9		
352.9+11.4	K 2-16	s 40		0.8 x 0.7		0.9 x 0.8	26.6 x 24.3		
355.1-06.9	M 3-21	s 59	1.7 x 1.4	1.5 x 1.8	2.6 x 1.9	1.6 x 1.8	4.4 x 3.9	15.5 x 13.7	0.1
355.4-04.0	Hf 2-1	g 9	9.5 x 7.0	2.0 x 1.6	10.4 x 8.5	2.1 x 1.9	18.1 x 14.9		
356.5-02.3	M 1-27	s 54	4.0 x 4.0	1.6 x 1.5	3.6 x 3.6	1.7 x 1.4	7.3 x 7.0		
356.7-06.4	H 1-51	g 3		1.9 x 1.7	9.2 x 9.0	2.0 x 1.6	18.0 x 15.5		
357.0+02.4	M 4- 4	s 48	3.4 x 1.7	0.8 x 0.8	3.2 x 3.5	0.8 x 0.8	6.4 x 5.3		
357.1-04.7	H 1-43	g 13	1.0 x 0.8	2.0 x 1.9	2.0 x 1.8	1.7 x 1.7	4.3 x 4.0		
357.3+04.0	H 2- 7	s 47	2.8 x 2.6	1.0 x 0.9	2.7 x 2.4	1.1 x 1.0	5.9 x 4.8		
357.6-03.3	H 2-29	s 56	9.9 x 5.9	1.0 x 1.1	6.0 x 5.9	1.0 x 1.1	10.9 x 10.0		
357.9-03.8	H 2-30	s 57	7.3 x 6.2	1.4 x 1.3	6.2 x 4.2	1.3 x 1.2	13.5 x 13.5		
358.3-21.6	IC 1297	s 79	7.3 x 3.5	0.8 x 1.0	6.2 x 6.6	0.8 x 0.9	10.9 x 9.9	19.0 x 18.5	0.2
358.5+05.4	M 3-39	g 29		1.7 x 1.7	10.6 10.3	1.6 x 1.8	26.1 x 18.4		
358.5-07.3	NGC 6563	s 63		1.5 x 1.5		1.7 x 1.5	59.2 x 43.2	80.5 x 48.0	2.1
358.6+01.8	M 4- 6	s 50	1.5 x 1.4	1.0 x 1.0	1.4 x 1.4	1.1 x 1.1	3.1 x 2.9		
358.6-05.5	M 3-51	g 10		2.1 x 1.7	7.8 x 7.7	2.1 x 2.1	21.2 x 14.8		
358.9-00.7	M 1-26	s 54	3.7 x 3.5	2.1 x 2.0	3.7 x 3.6	2.2 x 2.0	7.5 x 7.0	19.8 x 19.0	0.1
359.0-04.1	M 3-48	s 58	2.9 x 2.6	1.4 x 1.6	3.1 x 2.5	1.5 x 1.7	6.0 x 5.2		
359.1+15.1	A 40	s 40		0.9 x 0.8		0.9 x 0.9	34.3 x 30.4		
359.2+01.2	19W32	s 51		1.8 x 1.6		1.7 x 1.5	23.8 x 6.4		
359.3-00.9	Hb 5	s 55		1.4 x 1.2		1.6 x 1.3	51.7 x 18.3	60.1 x 27.8	0.9
359.4-03.4	H 2-33	s 58	5.3 x 5.0	1.6 x 1.4	3.9 x 3.4	1.6 x 1.3	8.3 x 7.8		
359.9+05.1	M 3- 9	s 48		0.8 x 0.8	9.0 x 7.5	0.8 x 0.9	17.3 x 15.2		